ANTIMICROBIAL ASSESSMENT USING SYNTHESIZED BINARY METAL OXIDE NANOPARTICLES.

BY

AWODERU SEGUN SAMUEL
PSC2105212

DEPARTMENT OF CHEMISTRY
FACULTY OF PHYSICAL SCIENCES
UNIVERSITY OF BENIN
BENIN CITY

OCTOBER 2025

ANTIMICROBIAL ASSESSMENT USING SYNTHESIZED BINARY METAL OXIDE NANOPARTICLES.

BY

AWODERU SEGUN SAMUEL

PSC2105212

BEING A PROJECT SUBMITTED TO THE DEPARTMENT OF CHEMISTRY IN PARTIAL FULFILMENT OF THE REQUIREMENT FOR THE AWARD OF A BACHELOR OF SCIENCE B.SC (HONS) DEGREE IN CHEMISTRY,

DEPARTMENT OF CHEMISTRY, FACULTY OF PHYSICAL SCIENCE, UNIVERSITY OF BENIN, BENIN CITY

OCTOBER 2025

CERTIFICATION

This is to certify that this project work was carried out by AWODERU SEGUN SAMUEL in the Department of Chemistry, University of Benin, Benin City, under the guidance and supervision of Mrs. Oluchi F. Emeribe.

_____ _____

Awoderu Segun S. **Date**

Project Student

_____ _____

Mrs. Emeribe F. Oluchi **Date**

Project Supervision

_____ _____

Prof. E.E. I. Irabor **Date**

Head of Department

DEDICATION

This project work is dedicated to God Almighty for His Grace and Mercies throughout the course of this Program and to my parents, Mr. and Mrs. Idowu Awoderu, for their love and prayers.

ACKNOWLEDGEMENT

I would like to sincerely extend my deepest appreciation to my project supervisor, Dr. (Mrs.) Emeribe, for her invaluable support, motivation, and constructive feedback throughout this research endeavor. My heartfelt thanks also go to Prof. E. E. Irabor, the Head of Department, for his guidance and support.

I am extremely thankful to my cherished parents, Mr. and Mrs. Idowu Awoderu, for their prayers, encouragement, and steadfast support. I would like to give special thanks to Dr. Oduwole for his generous financial support, which played a significant role in the success of this project.

Moreover, I acknowledge my brother, friend, and source of inspiration, Mr. Paul Shafe, for his ongoing motivation and encouragement. I am grateful to Mrs. Abijo, who has been like a mother and a tremendous supporter, as well as to other sponsors who contributed in various ways.

Lastly, I want to express my appreciation to my project partners (Alimikhena Marvellous and Igbagbeke Sarah) and classmates, Otunji Barnabas, Iyare Favour, and Anita Chinanu, just to mention a few, for their collaboration, moral support, and contributions, which helped make this project successful.

TABLE OF CONTENTS

LIST OF TABLES

LIST OF PLATES

LIST OF FIGURES

Fig. 1 .6 and 1.7 show a schematic diagram of a laser ablation chamber equipped with a rotating target holder

Fig. 1.8 showing an electron bright field image of gold nanorods

Fig 1.9 showing a typical green synthesis for different NPs

Abstract:

The growing global concern of antimicrobial resistance has fueled the hunt for alternative nanomaterials with therapeutic promise. This work used a green approach to create manganese–magnesium binary oxide (Mn–MgO) nanoparticles. *Ficus exasperata* leaf extract in alkaline environments (pH 9–10) act as a stabilizing and reducing agent. The nanoparticles' crystalline structure was validated by X-ray diffraction (XRD) examination, with distinctive peaks at 2θ values of 29.4°, 42.9°, and 62.0°, with an average crystallite size of 18 nm determined by the Debye–Scherrer equation. FTIR (Fourier Transform Infrared) spectrum showed notable peaks at 3339.69 cm^{-1} (O–H stretching), 1543.11 cm^{-1} (amide/aromatic C=C), and 1017.50 cm^{-1} (C–O stretching), suggesting the existence of capping agents made of phytochemicals. Highly aggregated, irregular particles were found using scanning electron microscopy (SEM) that created a porous cluster structure.

Energy Dispersive X-ray Spectroscopy (EDS) was used to verify the elemental composition; manganese (51.40 wt%), magnesium (35.00 wt%), and oxygen (5.20 wt%) were the primary elements. A primarily mesoporous structure was indicated by Brunauer–Emmett–Teller (BET) analysis, which showed a high specific surface area of 212.13 m^2/g, a total pore volume of 0.106 cm^3/g, and average pore diameters of 2.11 nm (BJH), 2.65 nm (DFT), and 3.04 nm (DA). A hybrid micro–mesoporous architecture was confirmed by the classification of the nitrogen adsorption–desorption isotherm as Type IV with an H3 hysteresis loop. There were no zones of inhibition (0 mm) against *Pseudomonas aeruginosa, Bacillus subtilis, Staphylococcus aureus, Escherichia coli, Aspergillus niger, and Candida albicans* when antimicrobial activity was assessed using the agar well diffusion method at doses ranging from 7.813 to 62.5 mg/mL. As a result, values for minimum bactericidal concentration (MBC) and minimum inhibitory concentration (MIC) were not determined. The Mn–MgO nanoparticles showed no discernible antibacterial activity despite having a large surface area and nanoscale crystallinity. This was probably caused by particle aggregation and surface passivation by phytochemical residues. These results demonstrate how important surface shape and accessibility are in influencing the bioactivity of green-synthesised nanoparticles.

Key: antibacterial, nanoparticles, green synthesis, binary metal oxides.

CHAPTER ONE: INTRODUCTION AND LITERATURE REVIEW

1.0 INTRODUCTION

“Nanotechnology, a term first clearly defined by Professor Norio Taniguchi of Tokyo Science University, refers to the manipulation of materials at the atomic or molecular scale. It involves the processing, separation, consolidation, distortion, and modification of matter at the nanometer level, typically with sizes below 100 nm. As a multidisciplinary field, nanotechnology has become a cornerstone of modern scientific innovation, encompassing material science, engineering, biology, and chemistry (Mansoori, 2005). Its remarkable development has opened new frontiers in surface-enhanced Raman scattering (SERS), nanobiotechnology, quantum dots, and microbial applications (Dvir *et al*., 2011).

Nanoparticles, characterized by their high surface-to-volume ratio and extremely small dimensions, exhibit properties significantly different from their bulk counterparts. These unique features render them suitable for diverse applications across electronics, optics, catalysis, biomedical science, and environmental technology (Ray, 2010; Bakand *et al*., 2012).

The concept of "Green Chemistry" for sustainable development has gained momentum over the past decade and a half. Sustainable development emphasizes meeting present needs without compromising the ability of future generations to meet theirs (Robert *et al*., 2005). Within the realm of chemical sciences, this entails minimizing environmental damage and optimizing the use of natural resources (Clark and Macquarrie, 2008; Omer, 2008). Traditional chemistry is often associated with hazardous substances, but the principles of green chemistry strive to minimize risks through safer material design and processes (Wilson and Schwarzman, 2009; Anastas and Eghbali, 2010).

Nanostructured metal oxides are gaining recognition for their distinct physicochemical and biological characteristics, which differ considerably from those of their bulk counterparts. At the nanoscale, attributes such as an increased surface-to-volume ratio, elevated surface energy, and effects of quantum confinement enhance their reactivity, catalytic efficiency, and biological interactions (Raliya & Tarafdar, 2014). These properties render them promising candidates for applications in biomedicine, specifically in the creation of antimicrobial agents.

Binary metal oxides merge two different oxides to produce synergistic effects that exceed the capabilities of single oxides. Manganese dioxide (MnO_2) is recognized for its oxidative capacity and its ability to produce reactive oxygen species (ROS), making it effective in disrupting microbial membranes and their internal components (Kumar *et al*., 2020). Conversely, magnesium oxide (MgO) is well-known for its biocompatibility, stability, and broad-spectrum antimicrobial efficacy (Krishnamoorthy *et al*., 2012).

The green synthesis of nanoparticles has emerged as an environmentally friendly alternative to traditional physical and chemical methods. Plant extracts, such as those from the leaves of *Ficus exasperata,* are abundant in bioactive compounds like flavonoids, phenols, alkaloids, saponins, and proteins, which act as natural reducing and capping agents (Kobelnik *et al*., 2021). This sustainable approach eliminates the need for harmful chemicals and results in nanoparticles that are coated with phytochemicals, thereby boosting their antimicrobial efficacy through synergistic interactions.

The antimicrobial efficacy of nanoparticles is significantly affected by their physicochemical characteristics. Binary manganese–magnesium oxide nanoparticles can enhance antimicrobial

effectiveness by improving charge transfer, surface reactivity, and the generation of reactive oxygen species (ROS), which results in a greater inhibition of bacterial and fungal growth. Smaller nanoparticles with larger surface areas enable more efficient interaction with microbial membranes, while specific crystalline structures can increase ROS production and enhance adhesion to cell walls. To comprehend these properties thoroughly, characterization methods such as X-ray diffraction (XRD), Fourier-transform infrared spectroscopy (FTIR), scanning electron microscopy (SEM), transmission electron microscopy (TEM), and Brunauer–Emmett–Teller (BET) surface area analysis are crucial. These methods provide valuable information about size, morphology, crystallinity, surface chemistry, and phytochemical functionalization.

The significance of this research is highlighted by the global issue of infectious diseases. Despite progress in antibiotics, the widespread misuse of broad-spectrum medications has led to an increase in antimicrobial resistance, diminishing treatment efficacy and raising mortality rates (Song *et al*., 2018). Nanoparticles, with their distinctive antibacterial mechanisms, present a promising option for combating drug-resistant pathogens (Jobby *et al*., 2018). Recent investigations have indicated that metal oxide-based nanoparticles have notable antimicrobial properties, making them appealing candidates for applications in biomedical fields, food preservation, and environmental sanitation (Selim *et al*., 2021).

Magnesium oxide (MgO) specifically has garnered interest because of its wide band gap (7.8 eV), thermodynamic stability, high surface reactivity, and low toxicity (Salem *et al*., *2019*). At the nanoscale, MgO demonstrates increased bactericidal activity, making it suitable for therapeutic applications such as biological labeling, wound dressings, and medical coatings. Moreover, the combination of MgO with manganese oxide (MnO_2) in a binary nanoparticle system has the potential to enhance surface area, improve photocatalytic activity, and increase antimicrobial efficiency (Hamza *et al.*, 2021).

As a result, this study examines the green synthesis, structural characterization, and antimicrobial assessment of MnO_2–MgO binary oxide nanoparticles produced using *Ficus exasperata* leaf extract. By investigating their effectiveness against bacterial and fungal pathogens, this research aspires to contribute to the advancement of eco-friendly, plant-derived nanomaterials with practical applications in healthcare, food safety, and environmental management.

1.1 BACKGROUND OF STUDY

Nanostructured metal oxides are gaining recognition for their distinct physicochemical and biological characteristics, which differ considerably from those of their bulk counterparts. At the nanoscale, attributes such as an increased surface-to-volume ratio, elevated surface energy, and effects of quantum confinement enhance their reactivity, catalytic efficiency, and biological interactions (Raliya & Tarafdar, 2014). These properties render them promising candidates for applications in biomedicine, specifically in the creation of antimicrobial agents. Manganese dioxide (MnO_2) is recognized for its oxidative capacity and its ability to produce reactive oxygen species (ROS), making it effective in disrupting microbial membranes and their internal components (Kumar *et al*., 2020). Conversely, magnesium oxide (MgO) is well-known for its biocompatibility, stability, and broad-spectrum antimicrobial efficacy (Krishnamoorthy *et al*., 2012). Thus, the integration of MnO_2 and MgO into a binary oxide system might improve

antimicrobial functionality by enhancing charge transfer, surface reactivity, and ROS generation, leading to greater inhibition of both bacterial and fungal pathogens. Eco-friendly and cost-efficient green synthesis methods utilizing plant extracts present an alternative to traditional physical and chemical nanoparticle fabrication techniques. This method not only avoids the use of harmful chemicals but also produces nanoparticles coated with phytochemicals, which may enhance antimicrobial effectiveness through synergistic interactions.

1.2 Statement of Problem

The swift rise of antimicrobial resistance (AMR) has made many traditional antibiotics less effective, presenting a major risk to global health (WHO, 2020). This issue has led to the exploration of new antimicrobial agents that are both effective and environmentally friendly. Nanotechnology has introduced new possibilities in this area, with metal oxide nanoparticles showing a wide range of antimicrobial activity through mechanisms that differ from those of traditional antibiotics, thus lowering the chances of resistance emergence (Krishnamoorthy *et al.,* 2012). Moreover, the fabrication of nanoparticles is frequently performed using traditional chemical or physical techniques that involve hazardous chemicals, considerable energy consumption, and non-biodegradable waste, which raises concerns about safety for the environment and biomedical applications (Mittal *et al.,* 2013). In light of this, green synthesis methods that utilize plant extracts as reducing and stabilizing agents are being investigated as eco-friendly, economical, and sustainable options. Although various plants have been utilized in the biosynthesis of nanoparticles, limited research has been conducted on using *Ficus exasperata* leaf extract, a plant reputed for its antimicrobial and medicinal qualities, for the green synthesis of MnO_2-MgO binary oxide nanoparticles. Additionally, there is sparse information regarding the morphological properties and antimicrobial effectiveness of such environmentally synthesized binary oxides against pathogenic microorganisms. Consequently, there is a significant research gap concerning the environmentally friendly synthesis and antimicrobial assessment of MnO_2–MgO binary oxide nanoparticles made from *Ficus exasperata* leaf extract. Filling this gap could pave the way for developing sustainable and effective antimicrobial agents that can combat resistant microbial strains, thereby enhancing public health and environmental safety.

1.3 JUSTIFICATION

The utilization of *Ficus exasperata* leaf extract for the production of nanoparticles is particularly important, as this plant is traditionally acknowledged for its medicinal and antimicrobial characteristics, yet its potential in nanomaterial research remains largely underexplored. Using *Ficus exasperata* not only promotes an environmentally friendly synthesis technique but may also improve the antimicrobial properties of the resulting MnO_2–MgO binary nanoparticles due to the interaction between bioactive phytochemicals and metal oxides.

- Consequently, this study is warranted as it aims to create a sustainable method for the synthesis of MnO_2–MgO binary oxide nanoparticles.
- Aid global initiatives against antimicrobial resistance (AMR) by developing alternative antimicrobial agents that are less toxic and more effective.

This research is anticipated to offer new perspectives on the synthesis and use of binary oxide nanoparticles, potentially benefiting biomedical, pharmaceutical, and environmental fields.

1.4 AIM OF RESEARCH

To synthesize manganese–magnesium binary oxide nanoparticles (Mn–Mg BO-NPs) using the leaf extract of *Ficus exasperata*, and assess their effectiveness in combating certain bacterial and fungal pathogens.

1.5 OBJECTIVES OF RESEARCH

The objectives of this research are to:

1. synthesize MnO–MgO nanoparticles utilizing *Ficus exasperata* leaf extract as an environmentally friendly reducing and stabilizing agent.
2. characterizing the produced nanoparticles through various spectroscopic and microscopic methods.
3. Assess the antimicrobial properties of the nanoparticles against specific bacterial and fungal strains.
4. contrasting the antimicrobial effectiveness of the combined MnO–MgO nanoparticles with that of individual MnO and MgO nanoparticles.

1.6 SCOPE OF STUDY

The main focus of this work is the green manufacture of binary metal oxide nanoparticles using plant extracts. The study's focus will be limited to particular plant species whose phytochemical components can serve as stabilizing and reducing agents during the creation of nanoparticles. The size, shape, crystallinity, and surface properties of the resultant nanoparticles will be evaluated using recognized analytical techniques.
The study will look into one main use for the produced material: the antibacterial efficacy using common microbiological testing techniques against specific bacterial and fungus strains.

The study will concentrate on a laboratory-based assessment of the materials' efficacy, laying the groundwork for potential scale-up and wider application in microbial management and environmental remediation.

1.7 LITERATURE REVIEW.

Nanoparticles, often referred to as ultrafine particles, are substances characterized by at least one dimension measuring between 1 and 100 nm, although in some cases, the definition may extend up to 500 nm. Particles that are smaller than 1 nm are classified as atomic clusters, while those that are larger fall into different categories: microparticles (1–1000 μm), fine particles (100–2500 nm), and coarse particles (2500–10,000 nm) (Salata *et al.,* 2004). The key trait of nanoparticles is their significant variation in physical and chemical properties when compared to bulk materials, which is primarily attributed to their diminutive size and elevated surface-to-volume ratio (Khan *et al*., 2019).

Due to their size being considerably smaller than the wavelength of visible light (400–700 nm), nanoparticles are not visible through optical microscopes; therefore, electron or laser microscopy is required for observation. When dispersed, nanoparticles often appear transparent because they do not scatter visible light like larger particles do (Horikoshi & Serpone, 2013). Moreover, they can pass through standard filters, which necessitates the use of specialized nanofiltration techniques for their separation (Roco *et al.,* 2011).

The distinct behaviors exhibited by nanoparticles primarily stem from surface effects. Since a significant proportion of their atoms are located at the surface (0.15–0.6 nm per atom), the properties of their surface prevail and often differ substantially from those of bulk materials. This phenomenon becomes even more significant when they are suspended in a medium of a different composition, where surface–interface interactions are essential (Bhattacharyya & Rinklebe, 2018). In terms of structure, nanoparticles have fewer point defects than bulk materials but demonstrate unique dislocation behaviors that affect their mechanical properties (Gleiter *et al*, 2000). They can be found in various shapes, including spherical and non-spherical forms (such as rods, cubes, and prisms), with shape-dependent anisotropy being crucial to their properties. For example, anisotropic gold, silver, and platinum nanoparticles display tunable optical resonance modes, which enable their use in applications like molecular labeling, biosensing, trace metal detection, and catalysis (Liz-Marzán *et al*., 2007).

Nanoparticles represent a middle ground between atoms/molecules and bulk substances, making them significant across various fields, including chemistry, physics, geology, and biology. They are found naturally in the environment and are also engineered in industrial settings, playing vital roles in a range of products from paints, plastics, and ceramics to biomedicine, catalysis, and environmental management (Singh *et al*., 2018). Their exceptional physicochemical characteristics-high surface reactivity, optical tunability, and mechanics influenced by defects-underpin modern nanotechnology and its expanding applications in industrial and biomedical fields.

1.8 Unique Properties Of Nanoparticles

Even when a substance is reduced down into micrometer-sized particles, its properties in nanoparticle form differ greatly from those of its bulk equivalent. The spatial confinement of subatomic particles (such as electrons, protons, and photons) and the surrounding electric fields are largely responsible for these variations. A significant factor at this size is also the high surface-to-volume-ratio.

Controlling Characteristics: A nanoparticle's properties are largely determined by the early phases of nucleation in the synthesis process. For example, nucleation determines the size of the nanoparticle. During the first stage of solid formation, a certain critical radius must be reached to prevent the particles from dissolving back into the liquid state.

Large Surface-Area-To-Volume Ratio: The surface area of particles weighing 1 kg with a volume of 1 mm^3 is equal to that of particles weighing 1 mg with a volume of 1 nm^3. Regardless of their size, bulk materials—those larger than 100 nm—are typically expected to have uniform physical characteristics like stiffness, density, viscosity, and thermal and electrical conductivity. Nanoparticles, on the other hand, react differently: the volume of the surface layer, which is only a few atomic diameters thick, represents a significant amount of the particle's overall volume; for particles with diameters of one micrometer or more, this proportion is insignificant. To put it another way, some properties of nanoparticles are more influenced by the ratio of surface area to volume than those of bulk particles.

Interfacial Layer: The interfacial layer, which is composed of ions and molecules from the medium that are placed within a few atomic diameters of each particle's surface, can change or mask the chemical and physical properties of nanoparticles suspended in a medium with different properties. In actuality, each nanoparticle's identity depends on this layer.

Solvent Affinity: Because the attraction forces between the particle surfaces and the solvent are strong enough to offset density changes that would normally cause a substance to either sink or rise in a liquid, solvent compatibility permits the production of nanoparticle suspensions.

Coating: Nanoparticles frequently acquire coatings composed of substances other than the particle's composition and the surrounding medium. The characteristics of the particles, such as their stability in suspension, catalytic activity, and chemical reactivity, can be dramatically changed by a coating that is only one molecule thick.

Diffusion Across the Surface: Because nanoparticles have a vast surface area, heat, chemicals, and ions can enter and exit them at remarkably high rates. Furthermore, the particles' small size allows the entire material to reach uniform equilibrium in terms of diffusion in a short period of time. As a result, many diffusion-dependent processes, such as sintering, can happen at lower temperatures and in shorter amounts of time, which can be important for catalytic activities.

Ferromagnetic and Ferroelectric Effects: Nanoparticles' small size affects their electrical and magnetic properties. Ferromagnetic materials at the micrometer scale are a prime example. Although these materials are frequently used in magnetic recording media because of the stability of their magnetic states, particles smaller than 10 nm are unstable and can change their state (flip) due to thermal energy at normal temperatures, making them unsuitable for such applications.

Magnetic Properties: The diminished vacancy density in nanocrystals can adversely impact the movement of dislocations, as the climb of dislocations necessitates the migration of vacancies. Furthermore, surface stress causes large internal pressure in small nanoparticles with strong curvatures. Similar to the effects seen during the work hardening process in materials, this creates a lattice strain that is inversely proportional to the particle size and is known to impede dislocation movement. Gold nanoparticles, for example, are significantly harder than their bulk counterparts. Furthermore, the possibility of dislocations interacting with the particle's surface is increased by the high surface-to-volume ratio in nanoparticles. This specifically affects the dislocation source's properties and permits dislocations to leave the particle before they can proliferate, which lowers the dislocation density and, as a result, limits plastic deformation.

There are particular difficulties in measuring mechanical qualities at the nanoscale since conventional techniques, such the universal testing machine, cannot be applied. As a result, new methods like nanoindentation have been created to supplement well-known scanning probe and electron microscopy methods. Hardness, elastic modulus, and the adhesion between the nanoparticle and substrate can all be evaluated by nanoindentation using atomic force microscopy (AFM). The force-displacement curves that arise from measuring the cantilever tip's deflection above the sample can be utilized to calculate the elastic modulus. It is still unclear, nevertheless, if the depth of indentation and particle size affect the elastic modulus values of nanoparticles as measured by AFM. Adhesion and friction forces are important considerations in nanofabrication, oiling, device design, colloidal stabilization, and drug delivery.

Melting Point Depression: When a substance is in nanoparticle form, its melting point may be lower than when it is in bulk form. For instance, bulk gold melts at 1064°C, yet 2.5nm gold nanoparticles melt at roughly 300°C.

Effects of Quantum Mechanics: Nanoscale materials exhibit quantum mechanics phenomena. These include superparamagnetism in magnetic materials, confined surface plasmons in certain metal particles, and quantum confinement within semiconductor particles. Quantum dots are semiconducting nanoparticles that are tiny enough—typically less than 10 nm—to display quantized electronic energy levels. The deep red to black hue of gold or silicon nanopowders and solutions is caused by quantum phenomena.

1.9 NANOTECHNOLOGY OVERVIEW

Over the past 20 years, nanotechnology—an interdisciplinary field—has made tremendous strides in tackling a wide range of issues in a variety of fields, including healthcare, environmental research, agriculture, food production, and other industries. Three primary techniques are used to create nanoscale materials (1–100 nm): chemical, physical, and biological processes. The synthesis can be accomplished in two ways: top-down and bottom-up. The reduction of bulk materials into smaller or nano-sized particles is referred to as the top-down technique, whereas the process of atom aggregation to create new nanomaterials is called self-aggregation or bottom-up.

Different processing materials and harsh circumstances, such as dangerous chemicals, pressure, adjusted pH, regulated temperature, and large equipment, are frequently required for chemical and physical production processes. In the end, these production processes are expensive and generate unwanted byproducts that may cause a number of environmental problems. The biological approach, on the other hand, is renowned for being quick, easy, eco-friendly, and more economical than chemical and physical procedures. As a result, scientists are concentrating more on biological or green processes that produce nanomaterials using bacteria, fungus, actinomycetes, algae, yeast, and plants.

The synthesis of nanoparticles, such as Ag, Au, Cu, CuO, ZnO, Fe2O3, TiO2, MnO, MgO, and others, utilizing biological methods has significantly increased recently. Compared to other metal nanoparticles, metal oxide nanoparticles have extra advantages such improved chemical stability and less toxicity. Because of these advantages, metal oxides are favored for a number of uses in the biotechnological and biological domains. Magnesium oxide nanoparticles (Mg-NPs) are unique among metal oxide nanoparticles because of their remarkable qualities, which include enhanced stability in biological fluids, reduced toxicity to human and animal tissues, and

photocatalytic activities. Biocatalysts, superconductors, paints, optical imaging, anti-adhesion, and wastewater treatment are just a few of the many uses for MgO-NPs.

Antibiofilm, antifungal, antibacterial, antiviral, antitumor, anticancer, biosensors, heartburn treatments, molecular signaling, bone regeneration, reducing the effects of magnesium deficiency, and as additives to eradicate foodborne pathogens are just a few of their many biological uses. MgO-NPs are useful antibacterial agents with long-lasting effects because of their low volatility and capacity to tolerate high temperatures. Notably, the FDA has approved them as a harmless nano-compound. The goal of this study is to investigate the multifunctional properties of MgO-NPs made from Penicillium chrysogenum metabolites. Several analytical methods, such as UV-Vis spectroscopy, X-ray diffraction (XRD), transmission electron microscopy (TEM), dynamic light scattering (DLS), scanning electron microscopy with energy dispersive X-ray spectroscopy (SEM-EDX), Fourier-transform infrared spectroscopy (FTIR), and X-ray photoelectron spectroscopy (XPS), were used to investigate the physicochemical properties of these biosynthesized MgO-NPs. Furthermore, the biological characteristics of the biosynthesized MgO-NPs were evaluated, specifically their antibacterial activity against unicellular fungi and pathogenic Gram-positive and Gram-negative bacteria. The larvicidal, pupicidal, and repellent activities against the Anopheles stephensi malarial vector were also assessed.

1.10 Binary Metal Oxides

Binary oxides are nanomaterials that consist of a combination of two different metal oxides within one system. In contrast to single oxides (such as ZnO or TiO_2 individually), binary oxides are designed to take advantage of the complementary or synergistic effects present in both components. They often exhibit improved physical, chemical, and functional characteristics compared to their single-oxide equivalents (Murty *et al*., 2016).

1.10.1 Synergistic Properties Of Binary Oxides

The selection of binary oxides is based on their synergistic benefits that emerge when the two oxides collaborate to achieve enhanced performance.

Increased Photocatalytic Efficiency: One oxide may function as a charge separator, while the other serves as an electron trap, minimizing the recombination of electrons and holes. This boosts the production of reactive oxygen species (ROS), making them more effective at breaking down hydrocarbons.

Enhanced Antimicrobial Efficiency: Binary oxides frequently release various metal ions, which can more effectively disrupt microbial cell walls and hinder metabolic processes compared to single oxides. The combined generation of ROS from both oxides amplifies the antimicrobial impact.

Thermal and Structural Resilience: Certain oxides (such as TiO_2) offer remarkable stability, while others (like ZnO, CuO, MgO) enhance reactivity. Together, they yield durable and active nanomaterials.

Band Gap Modification: By blending two oxides, the band gap can be adjusted, allowing for photocatalysis driven by visible light instead of being restricted to UV light as seen with TiO_2.

1.10.2 INSTANCES OF BINARY OXIDES

- $ZnO–TiO_2$: TiO_2 is very stable and commonly utilized as a photocatalyst; however, it faces the issue of significant electron-hole recombination. ZnO enhances its performance by offering high electron mobility and promoting reactive oxygen species (ROS) generation. The combination of $ZnO\text{-}TiO_2$ leads to improved photocatalytic breakdown of dyes, hydrocarbons, and increased antimicrobial effectiveness.
- $MnO_2–MgO$: MnO_2 possesses strong redox characteristics, making it very effective for oxidative reactions. MgO has a large surface area, excellent adsorption capabilities, and is recognized for its antimicrobial properties. Consequently, the MnO_2-MgO binary system can effectively decompose pollutants while also preventing microbial proliferation.
- $CuO–TiO_2$ (employed in wastewater treatment due to its enhanced ability to absorb visible light).
- $ZnO–Fe_2O_3$ (used for dye degradation and antibacterial coatings).
- $CeO_2–TiO_2$ (applied in oxidative catalysis and improved stability).

1.11 GREEN SYNTHESIS OF NANOPARTICLES

Although there are many ways to create materials at the nanoscale, there are typically two main approaches: top-down and bottom-up synthesis (Figure 1.1). The bottom-up strategy concentrates on assembling individual atoms to generate larger nanomaterials, whereas the top-down approach breaks down larger bulk materials into nano-sized particles. Silver (Ag), gold (Au), selenium (Se), cadmium sulfide (CdS), lead sulfide (PbS), and iron oxide (Fe_3O_4) are examples of metallic nanomaterials that have advantageous properties for a variety of applications.(Sweeney *et al*. 2004). Nanomaterial synthesis can be divided into two categories: standard procedures and green technologies. Traditional nanomaterial production methods have some compelling advantages. These approaches can manufacture a wide range of nanoparticles with numerous applications. Some technologies enable great scalability and fine control over nanoparticle form, making them useful in enhanced battery conduction, electrical applications, targeted disease therapy, and energy storage and conservation. However, the severe detrimental implications of using these traditional procedures are obvious. The high reliance on organic solvents for the production of these nanomaterials poses significant neurobehavioral and reproductive concerns during the process. Furthermore, high-pressure and high-temperature circumstances can create hazardous working settings. Concerns about volatile vapors and excessive carbon dioxide emissions, which considerably contribute to the greenhouse effect, are high on the priority list for these syntheses. In conclusion, these old procedures offer irreparable risks to both researchers involved in the synthesis and the environment. The potential disadvantages far exceed the benefits of standard nanomaterial manufacturing processes. As a

result of these concerns, traditional synthesis methods have declined in popularity, paving the way for greener alternatives. Given the ongoing climate catastrophe, it is critical to create creative approaches that follow the 12 Principles of Green Chemistry (Gimeno Fabr. *et al.,* 2018).

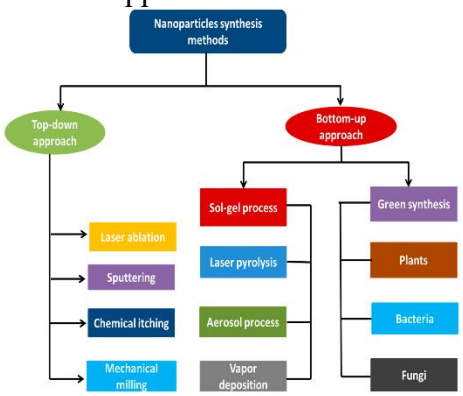

Figure 1.1 Top-down vs. Bottom-up synthesis schemes.

Nanomaterials can be made using two different processes. Top-down synthesis is the process of breaking down bulk materials into monomers. Bottom-up synthesis is the process by which atoms react with other substrates to form the desired nanomaterials. Green synthesis is a clean, safe, cost-effective, and environmentally friendly method for producing nanomaterials. Bacteria, yeast, fungi, several algae species, and certain plants operate as substrates for green nanomaterial synthesis. Different active compounds and precursors, such as metal salts, influence the final shape and size of the nanoparticles. Furthermore, green synthesis has advantages for nanomaterials, such as antibacterial capabilities and natural reducing and stabilizing properties. The active chemicals present in the microorganisms utilized as substrates in green synthesis contribute to these properties—a recent discovery since Saratale, R., *et al*.'s most complete assessment of nanomaterials. Green organisms engaged in nanomaterial creation often contain enzymes, amino acid groups, proteins, or unique chemical structures.

1.12 CHEMICAL SYNTHESIS OF NANOPARTICLES.

Chemical synthesis for nanoparticles involves generating nanoscale particles from precursor materials by chemical processes in either liquid or gas phases, with bottom-up approaches being a popular method. Various chemical processes, such as sol-gel, precipitation, hydrothermal, solvothermal, and polyol synthesis, allow you to customize the size and shape of nanoparticles by adjusting the precursor solution and reaction conditions. For example, the sol-gel technique involves the hydrolysis and condensation of precursors in a solvent, resulting in the formation of a gel, whereas the polyol method uses a high-temperature polyol solvent to reduce metal salts and act as a capping agent, allowing for the controlled nucleation and growth of nanoparticles.

1.12.1 SOL-GEL TECHNIQUE

The sol-gel technique is a popular wet-chemical method for developing nanomaterials. This technology makes it easier to produce a variety of high-quality metal oxide-based nanomaterials. It is known as the sol-gel approach because, during the synthesis of metal-oxide nanoparticles, a liquid precursor transforms into a sol, which then transforms into a gel structure. Metal alkoxides

are traditional precursors used in the sol-gel process to synthesize nanomaterials. The sol-gel technique to nanoparticle creation usually consists of many steps. To create a sol, the metal oxide first undergoes hydrolysis in water or in alcohol.

Condensation then occurs, increasing the viscosity of the solvent and forming porous structures that are left to age. During the polycondensation or condensation phase, M-OH-M (hydroxo) or M-O-M (oxo) bridges occur, culminating in the formation of metal-hydroxo or metal-oxo polymers in solution. Aging continues the polycondensation process, resulting in structural, property, and porosity changes. During this aging process, porosity decreases and the distance between colloidal particles increases. Following the aging stage, the gel is dried, which removes water and organic solvents. Finally, calcination is used to create nanoparticles.

The type of the precursor, the rate of hydrolysis, aging time, pH, and the molar ratio of H2O to the precursor all have an impact on the end product produced by the sol-gel process. The sol-gel method is environmentally friendly and has various advantages, including the uniform nature of the material produced, a low processing temperature, and a simple methodology for creating composites and complicated nanostructures.

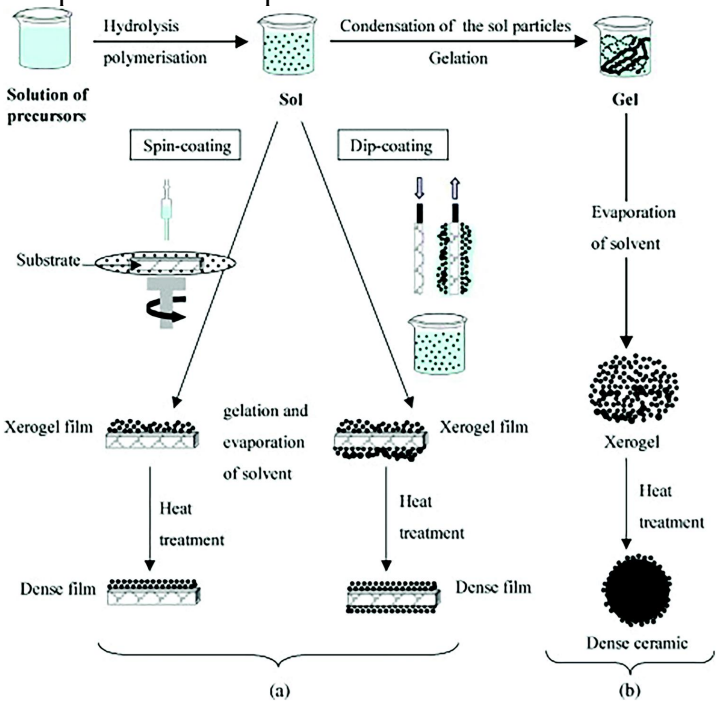

Fig 1.2 An overview showing two sol–gel method synthesis examples: (a) films from a colloidal sol and (b) powder from a colloidal sol transformed into a gel.

1.12.3 CHEMICAL REDUCTION METHOD

Chemical reduction, as the name implies, includes the application of chemical-reducing agents. This approach can be further classified based on the energy source used or the apparatus used for the reaction, resulting in a wide range of production possibilities. Chemical reduction is the most common and simple approach for creating nanoparticles out of the numerous chemical synthesis processes. The substrates used in this approach can be natural compounds obtained from plants or microbes, or reagents/chemicals capable of reducing materials from an oxidized state. Furthermore, nanoparticles made from natural materials tend to be less harmful than those made with chemical agents. The exact control over nanoparticle size, which allows the manufacture of nanoparticles with different morphologies, is an important element of chemical reduction synthesis. Furthermore, this technology is inexpensive and easily scaled up for greater output without requiring high pressure, energy, or temperature. Because of its simplicity, the principal chemical process for producing metal nanoparticles is the reduction of metal ions in solution. In reality, Michael Faraday was the first to perform systematic studies on the formation of colloidal gold using the chemical reduction approach as early as 1857. The chemical reduction process can take place in both aqueous and organic solvents, with the latter being the preferred choice. Metal nanoparticles must be carefully selected since they are particularly susceptible to oxidation. Adjusting the reaction conditions makes it possible to manufacture metal nanoparticles with certain dimensions, shapes, and distributions. Metal nanoparticles are synthesized by chemical reduction, which includes transforming metal salt complexes with a reducing agent and a stabilizer. The stabilizer's job is to prevent the metal nanoparticles from aggregating into bigger aggregates. Figure1.4 depicts the three main phases of a typical nanoparticle synthesis technique. In the first stage, a redox reaction occurs, in which electrons from the reducing agent are transferred to the metal atoms, resulting in the formation of free metal atoms. The formula for electron transfer from the reducing agent to the metal is as follows:

$$m\mathrm{Me}^{n+} + n\mathrm{Red} \rightarrow m\mathrm{Me}^{0} + n\mathrm{Ox} \qquad (1)$$

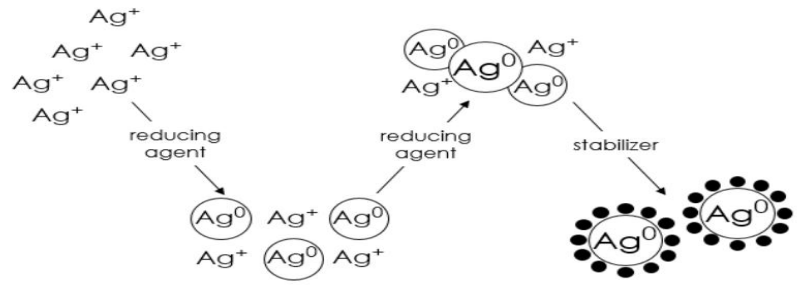

Fig 1.4: Scheme of nanoparticle formation (using silver as an example) by chemical reduction.

1.13 PHYSICAL METHODS OF SYNTHESISING NANOPARTICLES

1.13.1 PHYSICAL VAPOUR DEPOSITION (PVD)

PVD is a flexible synthesis technology that may produce thin film materials with nanometer-level control by carefully monitoring production variables. PVD is the process of generating vapour phase through evaporation, sputtering, laser ablation, or the use of an ion beam. Evaporation removes atoms from a source by heating it above its melting point. Sputtering, on the other hand, involves the ejection of atoms from the target surface due to the impact of energetic ions. Thermal evaporation has a constraint in multicomponent materials because one of the metallic elements usually evaporates first, due to variations in boiling point and vapour pressure between the evaporating species. Sputtering, on the other hand, can deposit materials with high melting points, such as refractory metals and ceramics, which are difficult to convert to nanostructures through evaporation. Sputtering, as opposed to evaporation procedures, can provide superior stoichiometric control over the film. Sputter-grown films are usually denser than evaporation-grown films because the sputtered atoms have more energy than the evaporated atoms. Sputtered films are more susceptible to contamination than evaporated films due to the poorer purity of the sputtering target materials.

1.13.3 LASER ABLATION

Laser ablation is well known for providing improved control over the evaporation process by evaporating constituent portions of multicomponent materials in a very short period of time. This approach uses a strong pulsed laser beam to irradiate the subject of interest, causing atoms and clusters to evaporate. The ablation rate refers to the total mass ablated from the target per laser pulse. Laser ablation in conjunction with IGC is an appealing way to produce bigger amounts of multicomponent nanocrystalline materials. Figure 1.5 illustrates a common laser ablation setup. A laser pulse causes atoms to preferentially collide with helium gas, losing kinetic energy quickly. They gradually condense to form a cloud of tiny nanocrystalline clusters. In this approach, the rate of nanoparticle synthesis varies according to helium gas pressure and laser pulse energy. Several researchers used laser ablation and gas condensation to create metal nanoparticles, metal oxides, and metal carbide.

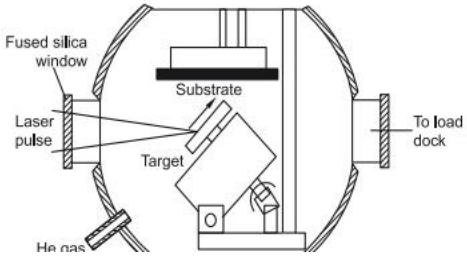

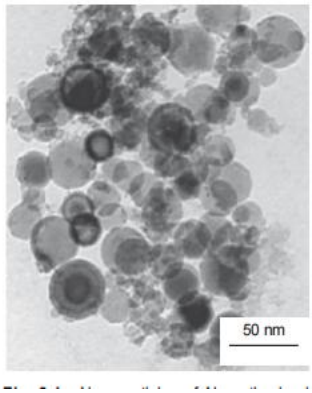

Fig. 1 .5 and Fig. 1 .6: A diagram of a laser ablation chamber with a spinning target holder and Al produced by wire explosion procedures.

1.13.5 CHEMICAL VAPOUR DEPOSITION

Chemical vapour deposition (CVD) is a method in which one or more gaseous adsorption species are utilized. On a heated surface, substances react or disintegrate to generate stable solids. The major steps that occur can be summarized as follows:

1. Transporting reactive gaseous species to the surface
2. Adsorption of the species onto the surface
3. The surface catalyzes heterogeneous surface reactions.
4. Surface dispersion of species to growth sites.
5. Film development and nucleation
6. Desorption and transfer of gaseous reaction products away from the surface.

CVD is a more difficult process of producing thin films and coatings than PVD. It has several distinguishing advantages, including the capacity to make highly pure and dense films or small particles at relatively high deposition rates, as well as the ability to coat complex-shaped components uniformly due to its non-line-of-sight nature. CVD deposits metallic, ceramic, and semiconducting thin films. Chemical reactions and deposition processes can be classified according to their activation sources. CVD is classified as thermally activated, laser-assisted, or plasma-assisted.

1.14 GREEN SYNTHESIS OF NANOPARTICLES

There are numerous varieties of nanoscale metals accessible, and they are used extensively in sectors such as biology, medicine, and engineering. For example, gold nanoparticles (Au NPs) are used in biology to regulate enzymes and show antibacterial and muscle relaxant characteristics (Islam et al., 2015). Silver nanoparticles (Ag NPs) have been shown to limit the growth and activity of gram-positive and gram-negative bacteria. Iron nanoparticles (Fe NPs) also inhibit bacterial development and are effective at remediating matrices contaminated with organic compounds, metals, nonmetal ions, and colors. Palladium nanoparticles (Pd NPs) have a variety of applications, including color degradation, antibacterial activity, and catalysis (Lebaschi *et al.,* 2017).

Currently, there is a growing body of research focused on the synthesis of nanoscale metals using chemical, physical, and green synthesis techniques (Wang *et al.,* 2007). Traditional, physical, and chemical methods are increasingly being supplanted by green synthesis methods due to concerns about excessive energy consumption, the release of toxic and harmful substances, and the requirement for complex equipment and synthesis conditions (Baruwati *et al.,* 2009). Aerosols, UV radiation, and thermal breakdown are three physical synthesis procedures that need high temperatures and pressures. To produce atomized aerosol droplets and nanoparticulate metals, the aerosol process, for example, requires a flame temperature of around 2400 K. Plasma-assisted physical vapor deposition produces PdO nanoparticles across three thermal cycles ranging from 250 °C to 800 °C, resulting in high energy expenditure. Chemical methods often rely on sodium borohydride, which is a costly and toxic reagent, along with other dispersant stabilizers and organic solvents (Hussain *et al.,* 2016). Green synthesis, on the other hand, uses natural and eco-friendly ingredients (such as reducing agents) that can also function as end-capping agents and dispersants, reducing energy requirements while also avoiding the use of poisonous and damaging agents. Green synthesis is currently primarily based on

microorganisms (fungi, bacteria, and algae) (Subramaniyam et al., 2015) or extracts derived from various plant parts, such as leaves (Devi *et al.,* 2019), flowers (Thovhogi *et al.,* 2016), roots, peels (Ehrampoush *et al.*, 2015), fruits, and seeds (Dhand *et al*., 2016; Gao *et al.,* 2016). Green materials contain polyphenols and proteins (Can, 2020) that act as reducing agents, changing metal ions to a lower valence state. Metal nanoparticles can be generated in the presence of these green components and under appropriate conditions (such as temperature, concentration, ambient air, and others).

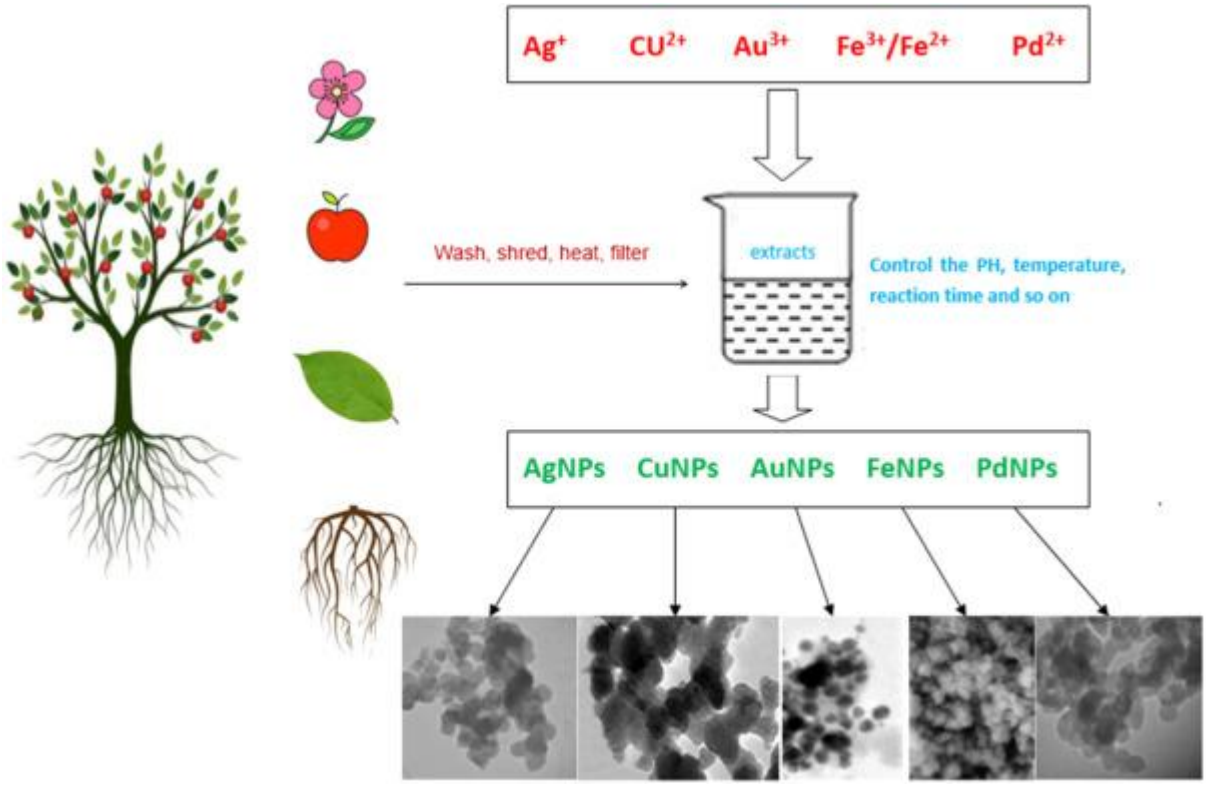

Fig 1.7 Showing a typical green synthesis for different NPs

Under specific circumstances, the quality of metal nanoparticles synthesized through green methods can even exceed that of those produced via chemical methods. For instance, the particle size of Fe3O4 nanoparticles synthesized using a green method ranges from 2 to 80 nm, considerably smaller than the 87 to 400 nm size range found in particles created through wet chemical methods (Gokila *et al*., 2021). Previous studies have underscored the benefits of green synthesis compared to chemical approaches and highlighted the potential and future prospects associated with green synthesis (Ren *et al*, 2019). Green synthesis presents several benefits when compared to traditional chemical and physical methods: it is non-toxic (Devi *et al.,* 2019), does not contribute to pollution (Alsammarraie *et al.,* 2018), is eco-friendly, cost-effective (Kataria and Garg, 2018), and more sustainable (Nasrollahzadeh and Mohammad Sajadi, 2016). Nonetheless, there are challenges related to the sourcing of raw materials, the duration of reactions, and the quality of the resultant products. For instance, the availability of raw materials

is limited (Turunc *et al.,* 2017), the synthesis process often takes a considerable amount of time (Subramaniyam *et al.,* 2015), and the product's particle size tends to be highly uniform (Gao *et al.,* 2016). This review collates the various processes involved in the green synthesis of nanomaterials and assesses the associated limitations. The aim of this review is to highlight the primary challenges and issues faced in the green synthesis of nanoscale metallic nanoparticles while suggesting future research directions. This review provides a more in-depth analysis and discussion of green synthesis, which could further enhance green research endeavors moving forward.

1.15 THE SIGNIFICANCE OF PLANT EXTRACTS IN THE SYNTHESIS OF NANOPARTICLES

Plant extracts are crucial in the eco-friendly synthesis of nanoparticles (NPs) thanks to the diverse range of secondary metabolites and biomolecules they encompass. These phytochemicals function in a dual capacity as reducing, capping, and stabilizing agents, thereby eliminating the necessity for external chemical reductants or surfactants that are usually employed in traditional synthesis methods.

- **As reducing agents:**

Compounds such as flavonoids, phenols, tannins, terpenoids, and alkaloids provide electrons or hydrogen atoms to transform metal ions (like Ag^{+}, Au^{3+}, Zn^{2+}, Mn^{2+}) into their elemental or oxide nanoparticle states (Mittal *et al*., 2013; Ahmed *et al.*, 2016). For instance, the presence of hydroxyl groups in flavonoids and phenolics enables them to chelate with metal ions, leading to oxidation and promoting the nucleation phase of nanoparticle production.

- **As capping agents**:

Following nucleation, phytochemicals such as proteins, polysaccharides, and polyphenols attach to the surface of nanoparticles via functional groups including –OH, $–NH_2$, –COOH, and –C=O. This adsorption creates a protective organic layer that inhibits uncontrolled growth and clumping (Makarov *et al*., 2014). This capping procedure is vital for controlling the size, shape, and dispersal of particles in aqueous environments. Tannins and proteins have been shown to effectively coat nanoparticles, stabilizing them through mechanisms of electrostatic repulsion and steric hindrance (Singh *et al.*, 2018).

- **As stabilizing agents:**

Phytochemicals contribute not only as capping agents but also by providing long-lasting colloidal stability, ensuring surface charge balance, and preventing the merging of nanoparticles (Kharissova *et al.,* 2013). The stabilizing impact is amplified when biomolecules establish robust hydrogen bonds or coordination complexes with the nanoparticle surface, a phenomenon observed with alkaloids and polyphenols (Ahmed *et al.,* 2016). Therefore, plant extracts act as an all-in-one system: the same biomolecules are responsible for reducing metal ions, capping the nanoparticles, and stabilizing the resulting colloid. This multifunctional nature illustrates why green synthesis is environmentally friendly, cost-efficient, and biocompatible, in contrast to chemical synthesis that necessitates distinct reducing agents (e.g., sodium borohydride) and stabilizers (e.g., polyvinylpyrrolidone) (Mittal *et al.,* 2013).

1.16 ANTIMICROBIAL ACTIVITY OF NANOPARTICLES

Nanoparticles (NPs) exhibit antimicrobial effects through mechanisms that are distinct from those of typical small-molecule antibiotics. Due to their minuscule size (1–100 nm), extensive surface area, and adjustable surface chemistry, NPs engage directly with microbial cells and produce chemical entities (such as reactive oxygen species and metal ions) that disrupt cellular structures and functions. This diverse mechanism of action minimizes the chances of microbes developing straightforward, single-target resistance, making NPs potential candidates as alternatives or supplements to traditional antimicrobials (Ikhuoria *et al* 2021; Uwidia *et al*, 2022).

Major Antimicrobial Mechanisms.

Several mechanisms can function concurrently; the dominant one is influenced by the NP's composition, size, shape, surface chemistry, and the environment.

- Generation of Reactive Oxygen Species (ROS): Numerous metal and metal-oxide NPs (such as TiO_2, ZnO, MnO_2, and CuO) facilitate the formation of ROS ($\bullet OH$, $O_2\bullet^-$, H_2O_2) through light-induced processes (photocatalytic) or in the absence of light (surface redox reactions). ROS can oxidize membrane lipids, proteins, and nucleic acids, leading to increased membrane permeability and enzyme deactivation. The simplified photocatalytic ROS pathway is:

$NP + h\nu \rightarrow e^- (CB) + h^+ (VB)$

$h^+ + H_2O \rightarrow \bullet OH + H^+$; $e^- + O_2 \rightarrow O_2\bullet^- \rightarrow H_2O_2 \rightarrow \bullet OH$

These radicals are extremely reactive and can kill bacteria. Even in dark conditions, certain oxides (like MnO_2) can engage in redox cycling to yield oxidants (Krishnamoorthy *et al*., 2012; Kumar *et al.,* 2020).

- Release of Metal Ions and Ionic Toxicity: Metallic NPs (such as Ag and Cu) or oxides can liberate metal ions (Ag^+, Cu^{2+}, Zn^{2+}) that target thiol groups in proteins, replace essential metal cofactors, and disrupt DNA replication. The release of ions is contingent upon NP solubility, pH, and surface chemistry; the presence of capping agents can hinder release (Mittal *et al.,* 2013).
- Direct Physical Contact and Membrane Disruption: Small NPs can attach to and infiltrate cell walls/membranes. Their binding changes the membrane potential, induces localized mechanical stress, and creates pores, resulting in the leakage of cellular contents. Nanoscale structures with high aspect ratios or sharp edges (such as some nanorods and nanoplates) can cause significant mechanical damage (Raliya & Tarafdar, 2014).
- Inactivation of Proteins and Enzymes: NPs might bind to enzymes and ribosomal components, obstructing vital metabolic pathways and protein synthesis. This could occur through direct surface interaction (metal-thiolate bonds) or oxidative modification via ROS/ions.
- Disruption of Quorum Sensing/Anti-Biofilm Activity: Certain NPs can interfere with cellular communication (quorum sensing) or limit the production of extracellular polymeric substances, which impedes biofilm creation or encourages biofilm dispersal. Inhibiting biofilm formation is particularly beneficial, as biofilms exhibit greater resistance to antibiotics.

- Photothermal/Photodynamic Effects (In Special Cases): Metal NPs (such as Au and some composites) can convert light into heat (photothermal) or initiate reactions with photosensitizers (photodynamic), thereby locally deactivating microbes upon irradiation.

1.16.1 FACTORS AFFECTING ACTIVITY RELATED TO MATERIALS AND ENVIRONMENT

- Composition: The specific elemental identity determines ion toxicity and redox behavior (for instance, Ag compared to MgO or MnO_2).
- Size: Smaller NPs typically possess a higher surface area and reactivity, penetrate cells more effectively, and often demonstrate stronger antimicrobial effects.
- Shape/Morphology: Edges, facets, and aspect ratios can affect membrane interactions and catalytic availability.
- Surface Chemistry/Capping: Organic capping (from environmentally friendly synthesis) can stabilize NPs, influence ion release, and contribute to antimicrobial activity (via phytochemicals). Zeta potential impacts electrostatic attraction towards microbial surfaces.
- Crystallinity and Defects: Crystal imperfections can serve as active sites for ROS generation.
- Aggregation State: Clumping reduces effective surface area and antimicrobial efficacy—dispersion capability is important.
- Dosage, Exposure Duration, and Medium Composition: Factors like ionic strength, pH, and organic materials in the testing medium affect NP stability, ion release, and ROS longevity. For example, elevated salt concentrations or proteins may interfere with NP–cell interactions or trap metal ions.
- Lighting Conditions: Photocatalytic materials need regulated illumination (wavelength and intensity) to facilitate ROS-mediated mechanisms.

1.16.2 Differences in Action Against Gram-Positive, Gram-Negative, And Fungi

Gram-negative bacteria possess an outer membrane composed of lipopolysaccharide that serves as a barrier, while also presenting negatively charged sites that can attract positively charged nanoparticles (NPs) or metal ions. In contrast, gram-positive bacteria feature a thicker layer of peptidoglycan but do not have an outer membrane; NPs that can disrupt the peptidoglycan physically or pass through its pores are effective in this case. Fungi are characterized by chitin-rich cell walls and typically necessitate higher concentrations of NPs; although the principal mechanisms remain reactive oxygen species (ROS) and membrane disruption, the kinetics may vary.

1.16.3 **How Antimicrobial Activity Is Measured**

Qualitative / Screening: Agar well diffusion or disc diffusion assays evaluate the size of the inhibition zone (mm). This serves as a useful initial screening method, although diffusion of NPs

through agar can be inadequate for large or agglomerated particles; it is not quantitative for insoluble NPs.

Quantitatively:

Minimum Inhibitory Concentration (MIC): This assay involves broth microdilution (MIC = the lowest concentration that halts visible growth). While valuable, one must be cautious of potential interferences from NPs in the assay (e.g., turbidity or dye adsorption).

Minimum Bactericidal Concentration (MBC): This involves plating samples from MIC wells to ascertain the reduction in viability (≥99.9%).

Time-kill (kinetic) assays: These examine colony-forming units (CFU) over time at specific NP doses to illustrate bactericidal kinetics.

Biofilm assays: These can include crystal violet staining, viable cell counts, or confocal microscopy to assess anti-biofilm effectiveness.

1.16.4 NANOPARTICLES FOR ANTIMICROBIAL ACTIVITY

Nanomaterials are substances with at least one dimension in the nanometer range (1-100 nm) or whose fundamental unit in three-dimensional space is on this scale. Nanoparticles, in particular, have demonstrated a broad variety of antibacterial activities against both Gram-positive and Gram-negative bacteria. For example, ZnO NPs have been demonstrated to inhibit Staphylococcus aureus, whereas Ag NPs exhibit concentration-dependent antibacterial action against Escherichia coli and Pseudomonas aeruginosa. However, the particular antibacterial actions of NPs remain imperfectly characterized, and identical forms of NPs can sometimes give contradictory responses. The antibacterial mechanisms attributed to NPs are commonly divided into three models: oxidative stress induction, metal ion release, and non-oxidative activities. These three mechanisms can function concurrently. Some studies suggest that Ag NPs neutralize the surface electric charge of bacterial membranes, altering their permeability and ultimately resulting in bacterial death. Furthermore, the generation of reactive oxygen species (ROS) impairs the antioxidant defense mechanisms and causes physical damage to the cell membrane. Bacterial infections cause a considerable number of chronic illnesses and deaths. Because of their low cost and efficacy, antibiotics have long been the preferred treatment for these infections. Nevertheless, multiple studies have demonstrated compelling evidence that the widespread use of antibiotics has resulted in the growth of multidrug-resistant bacterial strains. Indeed, antibiotic overuse has resulted in the emergence of superbugs, which are resistant to nearly all existing antibiotics. According to research, these bacteria have a super-resistance gene called NDM-1. The principal antibiotic classes currently used target three key bacterial functions: cell wall construction, translational machinery, and DNA replication machinery. Unfortunately, bacteria have the ability to evolve resistance to each of these strategies. Resistance mechanisms include producing enzymes that break down antibiotics, such as β-lactamases and aminoglycosides, modifying cellular components, such as the bacterial cell wall in vancomycin resistance and ribosomes in tetracycline resistance, and expressing efflux pumps that confer resistance to multiple antibiotics simultaneously.

Most antibiotic resistance strategies are ineffective against nanoparticles (NPs) because NPs interact directly with the bacterial cell wall, eliminating the need for cell penetration; this suggests that NPs may be less likely to cause bacterial resistance than antibiotics. As a result,

there has been a focus on developing novel NP-based materials with antibacterial properties. Many bacteria are found in biofilm formations, which are often made up of many species that interact with one another and their surroundings. Biofilms are microbial colonies that live on a solid substrate and produce extracellular products such as extracellular polymeric substances (EPSs). Bacteria can migrate onto surfaces momentarily, but the creation of EPSs causes their attachment to be persistent.

After settling, bacterial flagella development is inhibited, and the bacteria reproduce rapidly, resulting in the creation of a mature biofilm. At this time, the bacteria have formed a barrier that can survive antibiotics and act as a source of chronic infections. As a result, biofilms constitute a serious health concern. Furthermore, bacteria in biofilms can produce superantigens to avoid the human immune system. Thus, despite the availability of antimicrobial medicines and other modern antibacterial treatments, bacterial infections remain a substantial concern. Chronic infections caused by free-floating bacteria and biofilms are constantly difficult to treat because they have natural resilience to both antimicrobial treatments and the body's defenses.

Biofilms, in particular, are more resistant to antibacterial agents than planktonic microorganisms. Bacterial infections are a major hazard because they are the leading cause of chronic illnesses and mortality. Antibiotics have long been the preferred technique of treating bacterial illnesses due to their low cost and efficacy. However, multiple studies have shown that the widespread use of antibiotics has led in the rise of multidrug-resistant bacterial species. Indeed, super-bacteria, which are resistant to practically all known medicines, have recently emerged as a result of antibiotic abuse. These bacteria have been shown to contain a super-resistance gene known as NDM-1. Current antibiotics target three bacterial processes: cell wall construction, protein synthesis machinery, and DNA replication mechanisms.

As a result, research has focused toward novel nanoparticle-based materials with antibacterial capabilities. The majority of bacteria live in biofilms, which are generally made up of multiple species interacting with one another and their surroundings.

Certain researchers have investigated non-oxidative mechanisms to analyze the antibacterial properties of MgO nanomaterials using tools such as electron spin resonance, liquid chromatography-mass spectrometry, proteomics, transmission electron microscopy (TEM), Fourier transform infrared (FTIR), and flat cultivation. Under UV light, natural light, or complete darkness, three MgO NP versions have excellent antibacterial properties against E. coli. Three observations show that the antibacterial actions of these NPs are not connected with membrane lipid peroxidation generated by oxidative stress.

1. When the bacterial cell membrane is damaged and surface pores are visible, MgO NPs are not found inside the cell, and no significant Mg ions are discovered in the energy-dispersive X-ray spectroscopy spectra, showing that MgO's inhibitory effect affects the cell membrane.
2. Only one form of MgONP may generate trace quantities of ROS, while the other two cannot.
3. After treatment with MgONPs, the levels of lipopolysaccharide (LPS) and phosphatidylethanolamine (PE) in the cell wall alter negligibly, indicating that MgO does not produce lipid peroxidation. Furthermore, there is no increase in ROS-related proteins within the cell, but several key cellular metabolic activities associated with proteins, such as amino acid

metabolism, glucose metabolism, energy metabolism, and nucleotide metabolism, are drastically reduced.

Ramesa et al. (2018) investigated the manufacture of silver nanoparticles from Azadirachta indica leaves, as well as the effects on Staphylococcus aureus growth and glutathione-S-transferase activity. The nanoparticles were made biologically and examined using SEM, XRD, UV spectrophotometry, DLS, TEM, and FTIR. The UV-Vis absorbance spectra of the nanoparticles revealed a distinct peak at 420 nm, showing that the AgNO3 produced may push the greatest absorption peak into the visible light range. The particle size distribution of the produced nanoparticles was assessed using dynamic light scattering (DLS). The polydispersity index was discovered to be 0.373%. The antibacterial capabilities of the produced nanoparticles were investigated, and it was determined that the particles may target specific bacteria by penetrating the cell membrane and affecting their respiratory activity.
Shrivastava *et al.* (2007) produced silver nanoparticles (AgNPs) and shown their significant antibacterial activities against Escherichia coli, Staphylococcus aureus, and Pseudomonas aeruginosa. The results showed that AgNPs were particularly efficient against Gram-negative bacteria such as E. coli. This efficacy is attributed to Gram-negative bacteria's thinner peptidoglycan coating and higher negative surface charge, which increase electrostatic attraction to silver nanoparticles (Morones *et al.,* 2005).
Raghupathi *et al.* (2011) investigated the antibacterial activities of ZnO nanoparticles against different bacterial species, including Escherichia coli (Gram-negative) and Staphylococcus aureus (Gram-positive). Their findings revealed that smaller ZnO nanoparticles (less than 50 nm) have significantly higher antibacterial activity than larger particles. This increased activity was attributed to their higher surface-to-volume ratio, which enabled more efficient interactions with bacterial cells. Magnesium oxide nanoparticles are appealing because they are biocompatible, inexpensive, and environmentally safe. Krishnamoorthy *et al*. (2012) found that MgO NPs have antibacterial properties against E. coli and S. aureus, resulting in a considerable reduction in bacterial growth. The hypothesized mechanism includes the production of reactive oxygen species (ROS), an increase in local pH caused by MgO dissolution, and direct interaction with the cell wall, which results in cell membrane rupture and cytoplasmic material leakage (Jin & He, 2011).

MgO NPs are utilized in wound dressings, dental products, antimicrobial coatings, food preservation, and wastewater treatment, providing an environmentally friendly substitute for traditional antimicrobial agents (Makhluf *et al.,* 2005). Manganese oxide nanoparticles exhibit multiple oxidation states and possess catalytic characteristics, rendering them effective as antimicrobial agents. According to Chen *et al.* (2012), MnO_2 NPs were able to inhibit both Gram-positive (*S. aureus*) and Gram-negative (*E. coli*) bacteria through mechanisms that include the generation of reactive oxygen species (ROS), induction of oxidative stress, and disruption of membranes. Furthermore, the release of Mn^{2+} ions disrupts bacterial enzyme functions and metabolic processes (Zhang *et al.,* 2015). Applications of MnO_2 NPs include use in antibacterial coatings, drug delivery systems, environmental cleanup, and catalysis. Their capability to act as

"nanozymes" (mimics of enzymes) boosts their potential for antimicrobial actions and oxidative degradation (Sujana *et al.,* 2016).

Emeribe and Ebiaguanye in 2024, reported an innovative and environmentally sustainable method for synthesizing magnesium oxide nanoparticles (MgO NPs) using *Pennisetum purpureum* (elephant grass) extract as both a reducing and stabilizing agent. Their study emphasized that green synthesis methods are more cost-effective and eco-friendly compare to conventional chemical synthesis techniques.

1.16.5 ADVANTAGES AND LIMITATIONS OF NANOPARTICLES FOR ANTIMICROBIAL ACTIVITY

Advantages of nanoparticles as antimicrobial agents

1. Broad-spectrum antimicrobial efficacy: Nanoparticles are effective against a diverse array of pathogens, including both Gram-positive and Gram-negative bacteria, fungi, and even viruses (Rai *et al*., 2009).In contrast to traditional antibiotics, they function through various mechanisms (such as ROS generation, metal ion release, and disruption of cell walls), which reduces the likelihood of developing resistance.

2. Nanoscale size and increased surface area: Their small size (1–100 nm) enables them to infiltrate microbial cell walls and membranes more effectively than larger materials (Sirelkhatim *et al.,* 2015). A high surface-to-volume ratio boosts reactivity and antimicrobial efficacy.

3. Diverse modes of action: Nanoparticles target microbes through generating oxidative stress, releasing ions, interacting with proteins and DNA, and rupturing cell walls (Shrivastava *et al.,* 2007). This multifaceted strategy lowers the probability of bacteria acquiring resistance compared to single-target antibiotics.

4.Synergistic interactions with antibiotics: Research demonstrates that the use of nanoparticles (such as AgNPs and ZnO NPs) in conjunction with traditional antibiotics increases drug effectiveness and helps to combat multidrug resistance (Hajipour *et al.,* 2012).

5. Sustained stability and controlled release: Certain nanoparticles (like MgO and ZnO) show a gradual, sustained release of ions, which offers prolonged antimicrobial activity. This characteristic makes them ideal for applications such as coatings, wound dressings, and food packaging (Makhluf *et al.,* 2005).

6. Eco-friendly green synthesis enhances safety: The use of plant-based methods for synthesizing nanoparticles minimizes toxic by-products, while boosting biocompatibility, stability, and environmental sustainability (Mittal *et al*., 2013).

Limitations of Nanoparticles in Antimicrobial Applications

1. Possible cytotoxic effects on human cells: While efficient against pathogens, certain nanoparticles (notably AgNPs and ZnO NPs) can harm human cells and tissues at elevated concentrations due to oxidative stress and ion release (AshaRani *et al.,* 2009).

2. Environmental issues: The longevity of nanoparticles in soil and aquatic environments may result in bioaccumulation and toxicity, impacting marine life and beneficial microorganisms (Klaine *et al.,* 2008).

3. Emergence of nanoparticle resistance: Although rarer than antibiotic resistance, bacteria may develop tolerance to nanoparticles through mechanisms like biofilm formation, efflux pumps, or modifications of surface charge (Hajipour *et al*., 2012).

4. Expense of large-scale manufacturing: While green synthesis helps lower costs, achieving large-scale, standardized production of nanoparticles with uniform size and shape is still problematic and costly (Iravani, 2011).

5. Absence of standardized procedures: Variations in synthesis techniques (chemical, biological, physical) lead to discrepancies in size, shape, and surface characteristics, complicating the comparison of findings across different studies.

6. Uncertain long-term safety: The toxicological profile and potential long-term health consequences of exposure to nanoparticles in humans are not fully known, indicating the need for more in vivo research and clinical trials.

1.17 Characterization Methods For Nanoparticles

As previously stated, the morphological and topographical qualities of nanoparticles (NPs) are critical since they influence the majority of their properties. These properties include the size, shape, dispersity, localization, agglomeration/aggregation, surface morphology, surface area, and porosity of NPs. The following methods are routinely used to characterize the morphological and topographical properties of nanoparticles.

Electron Microscopy (EM) Techniques, SEM, STM, and TEM are commonly used to examine NP size, shape, and surface properties. In SEM, an electron cannon produces an electron beam that travels a predetermined path through a lens system before striking the sample. When the beam strikes the sample, it emits electrons and X-rays from its surface. Detectors then capture the dispersed electrons and X-rays, resulting in a 3D reconstruction of the material. SEM can provide a variety of characteristics regarding NPs, including their size, shape, aggregation, and distribution. Similarly, TEM provides insights into NP size, shape, localization, dispersity, and aggregation via two-dimensional imaging.

Scanning electron microscopy (SEM), scanning tunneling microscopy (STM), and transmission electron microscopy (TEM) are frequently used to determine NP size, shape, and surface properties. An electron gun in SEM generates an electron beam that travels a predetermined path through a lens system before striking the sample. When the beam strikes the sample, it emits electrons and X-rays from the surface. Detectors then capture the dispersed electrons and X-rays to create a three-dimensional reconstruction of the material. SEM may reveal a variety of characteristics regarding NPs, including size, shape, aggregation, and dispersal. Likewise, TEM gives insights into NP size, shape, localization, dispersity, and aggregation through two-dimensional imaging. STM operates on quantum tunneling principles, with a metallic tip placed close to the sample surface to apply voltage. This voltage extraction of electrons from the surface creates an electrical current, which is then used to recreate a high-resolution image of the surface. STM is largely used to study the topography of NPs. These approaches are particularly useful for determining the morphological properties of inorganic NPs. Organic NPs (or those with

biological coatings), on the other hand, frequently necessitate sophisticated sample preparation, making their application difficult. Such preparations may cause sample dehydration, leading in phenomena such as sample shrinkage and aggregation.

Dynamic Light Scattering (DLS): This technique is commonly used to determine the size and distribution of nanoparticles (NPs). It works by monitoring light interference caused by Brownian movement of NPs in suspension and using the Stokes-Einstein equation to correlate NP velocity (diffusion coefficient) with their size. The polydispersity index, calculated using an autocorrelation function, represents the range of NP size distribution. Polydispersity index values vary from 0 to 1, with 0 indicating total homogeneity and 1 indicating high heterogeneity. In addition, this method allows for the study of non-spherical NPs using multistage DLS. This is also known as photon correlation spectroscopy (PCS).

The Brunauer–Emmett–Teller (BET): This method is based on the adsorption and desorption concepts developed by Stephen Brunauer, Paul Emmett, and Edward Teller, and it is one of the most reliable techniques for determining the surface area of nanoparticles. In the BET analysis, a partial vacuum is established by chilling the surface with liquid nitrogen, which aids in the adsorption of nitrogen gas onto the sample. This approach takes use of the weak contacts between the solid and gaseous phases, allowing for quantifiable levels of adsorption. Once the adsorption monolayers have formed, the sample is removed from the nitrogen environment and heated to allow for the desorption and measurement of adsorbed nitrogen.

X-Ray Diffraction Analysis (XRD)

This technique entails aiming X-rays at a material and then measuring the intensities and scattering angles of the X-rays that exit. XRD is a widely used technique for determining the phase and crystallinity of nanoparticles. Nonetheless, XRD precision and resolution can be impaired when the samples are extremely amorphous with variable interatomic distances or when the NPs comprise fewer than several hundred atoms. The XRD examination of biogenic Ag NPs generated using Trichoderma koningii, Solanum tuberosum, and Acanthospermum hispidum leaf extract revealed distinctive peaks at roughly $2\theta = 38°$, 44°, and 64°, corresponding to the (111), (200), and (220) planes. These results are consistent with reference data for crystalline silver's face-centered cubic structure. However, the XRD results for Ag NPs produced from Solanum tuberosum were less distinct than those of other biogenic Ag NPs and contained various contaminants. The structural characterisation of Pd NPs generated from Garcinia pedunculata Roxb leaf extract by XRD revealed obvious peaks for Pd, but three additional peaks at 2θ values of 34.22˚, 55.72˚, and 86.38˚ were also identified, confirming the existence of PdO phases alongside the NPs.

Energy-Dispersive X-Ray Spectroscopy (EDX) is a technique that uses an electron beam to target a sample. When incident electrons impact the sample's surface, they can displace inner shell electrons, prompting outer shell electrons to migrate in and fill the vacancies, resulting in the emission of X-rays. Because of their unique atomic arrangements, each chemical element produces a characteristic X-ray emission pattern, allowing for compositional analysis. One disadvantage of EDX is that the generated spectra only provide qualitative compositional

information (showing the chemical constituents in the sample but not measuring them). Nonetheless, the intensity of the peaks can provide a rough approximation of an element's relative abundance in the sample. This method requires no complex extra equipment and is often a tiny device that connects to an existing scanning electron microscope (SEM) or transmission electron microscope (TEM).

Fourier-Transform Infrared Spectroscopy (FTIR): This method involves exposing a substance to infrared radiation and measuring the amount of light that is absorbed or transmitted. The resulting spectrum serves as a distinguishing fingerprint for the samples, disclosing information about their composition such as the types of bonds present, their polarity, and oxidation state. This method is typically used to analyze organic compounds, such as evaluating the surface chemical makeup or functionalization of nanoparticles. It also helps to discover impurities when high purity is sought.

1.18 IDENTIFIED RESEARCH GAP

Research Gap

Despite extensive research on the antimicrobial, photocatalytic, and environmentally friendly synthesis characteristics of MnO_2 and MgO nanoparticles, the majority of studies have concentrated on individual metal systems. There is limited understanding of binary MnO_2–MgO nanostructures, especially regarding their combined antimicrobial and photocatalytic properties under eco-friendly synthesis conditions. Although several plants such as *Azadirachta indica, Ocimum sanctum, Moringa oleifera, and Ficus carica* have been utilized for nanoparticle synthesis, *Ficus exasperata* has not been adequately investigated, despite its abundance of phytochemicals, including flavonoids, alkaloids, tannins, and phenols (Okoye *et al.,* 2014). Thus, there is a notable void in the green synthesis of binary MnO_2–MgO nanoparticles using *Ficus exasperata* extract and in assessing their antimicrobial properties. Addressing this void could lead to the development of innovative, plant-derived nanomaterials that may help combat antimicrobial resistance.

Chapter 2

2.0 Materials and Methods

2.1 Apparatus

- Beakers
- Stapula
- Crucibles
- Measuring cylinder
- Magnetic stirrer
- Round bottom
- Centrifuge
- pH meter
- Micropipette
- Incubator
- Autoclave
- Oven and furnace
- Characterization instruments: FTIR, SEM,XRD

2.2 REAGENTS USED

- Magnesium acetate
- Manganese acetate salt
- Distilled water
- 0.1M NaOH
- Plant extract
- Mueller Hinton agar
- Sterile water
- Bacillus subtilis,
- Staphylococcus aureus,
- Pseudomonas aeruginosa,
- Escherichia coli,
- Candida albicans, and
- Aspergillus niger

2.3 METHODOLOGY

2.31 Collection, Identification, and Preparation of Plant Samples

In Ugbowo, Benin City, Nigeria, fresh *Ficus exasperata* leaves were collected and identified by H. A. Akinnibosun of the Plant Biology and Biotechnology Department at the University of Benin and UBH-F319 is the herbarium voucher number. After properly cleaning the gathered leaves with distilled water to get rid of dust and impurities, they were allowed to air dry at room temperature. A cleaned milling machine running at 1200 rpm was used to grind the dried leaves into a fine powder, which was then kept in an airtight container for later usage. The plant extract was made by combining 500 mL of distilled water with 50 g of powdered leaves. The mixture was physically shaken and left overnight to ensure complete phytochemical extraction. After that, the extract was filtered to create a clear filtrate, which was stored in a clean container for the production of nanoparticles. 0.1 M of each precursor solution was made using manganese acetate tetrahydrate $(CH_3COO)_2Mn \cdot 4H_2O$ and magnesium acetate tetrahydrate $(CH_3COO)_2Mg \cdot 4H_2O$). After the mixed metal salt solution was fully dissolved, 200 mL of *Ficus exasperata* leaf extract was added. A magnetic stirrer was used to continuously agitate the reaction mixture for three hours. During this process, 0.1 M NaOH solution was added dropwise to encourage the nucleation and growth of the nanoparticles while maintaining the pH between 9 and 10 and promoting the formation of metal hydroxide precipitates. The precipitate was separated using a centrifuge set at 10,000 rpm for 10 minutes. After discarding the resultant supernatant, the precipitate was repeatedly cleaned with distilled water to get rid of any remaining contaminants. To obtain purified nanoparticles, the cleaned product was centrifuged for five minutes at 10,000 rpm. In order to remove organic residues and transform the intermediates into stable Mn–MgO binary oxide nanoparticles, the precipitate was first dried in an oven to remove moisture, and then it was calcined at a temperature of 300 degrees Celsius in a furnace. The completed product was stored in a clean, airtight container for further characterization and analysis.

Plate 2.1 showing the typical picture of *ficus exasperate* leaves.

Plate 2.2 showing the plates of Manganese and Magnesium acetate salt.

Plate 2.3 showing the precipitate of the nanoparticles

2.4 Phytochemical Screening.

Phytochemicals composition of the leaves was determined using the methods variously described by Trease and Evans(1996) and Sofowora (2006).

2.5 Characterization techniques used for characterizing NPs

The purified Nanoparticles of Mn-Mg binary metal oxides were used for the following characterization. FTIR (Fourier Transform Infrared Spectroscopy): Detects functional groups from the phytochemicals of *Ficus exasperata* that are involved in the capping and stabilization of nanoparticles, and verifies the elimination of organic residues after calcination. BET (Brunauer–Emmett–Teller analysis): Assesses the specific surface area, pore size, and pore volume of the nanoparticles, which are essential for their antimicrobial and photocatalytic properties. SEM (Scanning Electron Microscopy): Displays the surface characteristics, particle shape, and approximate size distribution of the nanoparticles. XRD (X-ray Diffraction): Validates the crystalline structure, phase composition, and average crystallite size of the synthesized Mn–Mg oxide nanoparticles.

2.6 ANTIMICROBIAL ACTIVITY TEST PROCEDURES

2.6.1 **Assessment of Antimicrobial Activity Using Diffusion Method in Agar Wells:**

- The antibacterial efficacy of the synthesized Mn–MgO was evaluated using the agar well diffusion technique. Binary oxide nanoparticles' efficacy against specific bacterial and fungal species was assessed.
- A nanoparticle stock solution was serially diluted to reach concentrations ranging from 62.5 mg/mL to 7.813 mg/mL.
- Mueller-Hinton agar (MHA) was produced according to conventional procedures and autoclaved at 121 °C for 15 minutes to sterilize it. About 30 mL of the sterilized media were added to aseptically filled sterile Petri plates, which were then left to harden. After that, any remaining moisture on the plates' surface was eliminated by drying them for 10 minutes at 50 °C in a convection oven.
- Test organisms were suspended in sterile normal saline, and the turbidity was adjusted to match the 0.5 McFarland standard to create microbial inocula that were cultured. Using a sterile swab, the standardized inoculum was evenly distributed over the agar surface.
- Using a sterile cork borer, wells with a diameter of 8 to 10 mm were aseptically drilled into the agar, and molten agar was used to seal each well's base. A calibrated micropipette was then used to gently add 0.2 mL of each nanoparticle concentration into the wells.
- The plates were incubated in an inverted posture at 37 °C for 24 hours after being left at room temperature for 30 minutes to allow the nanoparticles to diffuse.

CHAPTER 3: RESULTS AND DISCUSSIONS

3.1 Result of Phytochemical Screening.

The phytochemical composition of the leaves was determined using the methods variously described by Trease and Evans (1996) and Sofowora (2006).

Chemical Test	***Ficus Exasperata***
Tannis	++
Saponin	++
Flavonoid	++
Steroids	++
Terpenoids	++
Anthraquinones:	++
Reducing sugar	++

Legends: ++ Presence

3.2 Morphological and Elemental Analysis- SEM

The morphology of the binary nanoparticles composed of manganese and magnesium oxide is illustrated in Figure 3.1A-C. The size, shape, distribution, and elemental makeup of the plant-mediated manganese–magnesium oxide nanoparticles were examined using SEM and EDS. The findings suggest that the aqueous extract from *Ficus exasperata* effectively facilitates the formation of clusters of irregular, rough-edged primary particles, which tend to fuse or agglomerate into larger, porous aggregates. According to prior research carried out by Xiong *et al.* (2021), factors such as the concentration and volume of the extract, as well as the reaction temperature and pH, can greatly impact key characteristics, including particle size, shape, and levels of agglomeration. Figure 3 displays the SEM image of manganese–magnesium oxide nanoparticles, highlighting noticeable particle aggregates. The particles show a non-uniform, irregular, and agglomerated structure, along with a diverse size distribution. The arrangement consists of clustered flakes, rather than distinct spherical particles, which is typical of plant-mediated synthesis. This flake-like structure can be linked to the role of phytochemicals and other biomolecules during the reduction and stabilization processes. Similarly, the EDS spectrum provided in Figure 3.1D verifies the elemental composition of the biosynthesized manganese–magnesium oxide nanoparticles, thus confirming the successful incorporation of both metal oxides. The presence of clear peaks associated with magnesium, manganese, and oxygen within the binding energy range of 0.2–3.0 keV validates the successful formation of manganese–magnesium oxide nanoparticles. Furthermore, Figure 3.1D also illustrates that the primary elemental constituents of the Mg–Mn–O nanoparticles were found to be magnesium (35.00%), manganese (51.40%), and oxygen (5.20%) based on weight, affirming their successful synthesis. Minor signals of carbon (3.10%), sodium (2.10%), and ion (3.00%) were also detected, which can be attributed to phytochemicals most likely from *Ficus exasperata* extract, as well as potential contamination from glassware or salts used in the synthesis process. The results affirm

the high purity levels of magnesium, manganese, and oxygen, thereby confirming the successful green synthesis of magnesium–manganese oxide nanoparticles.

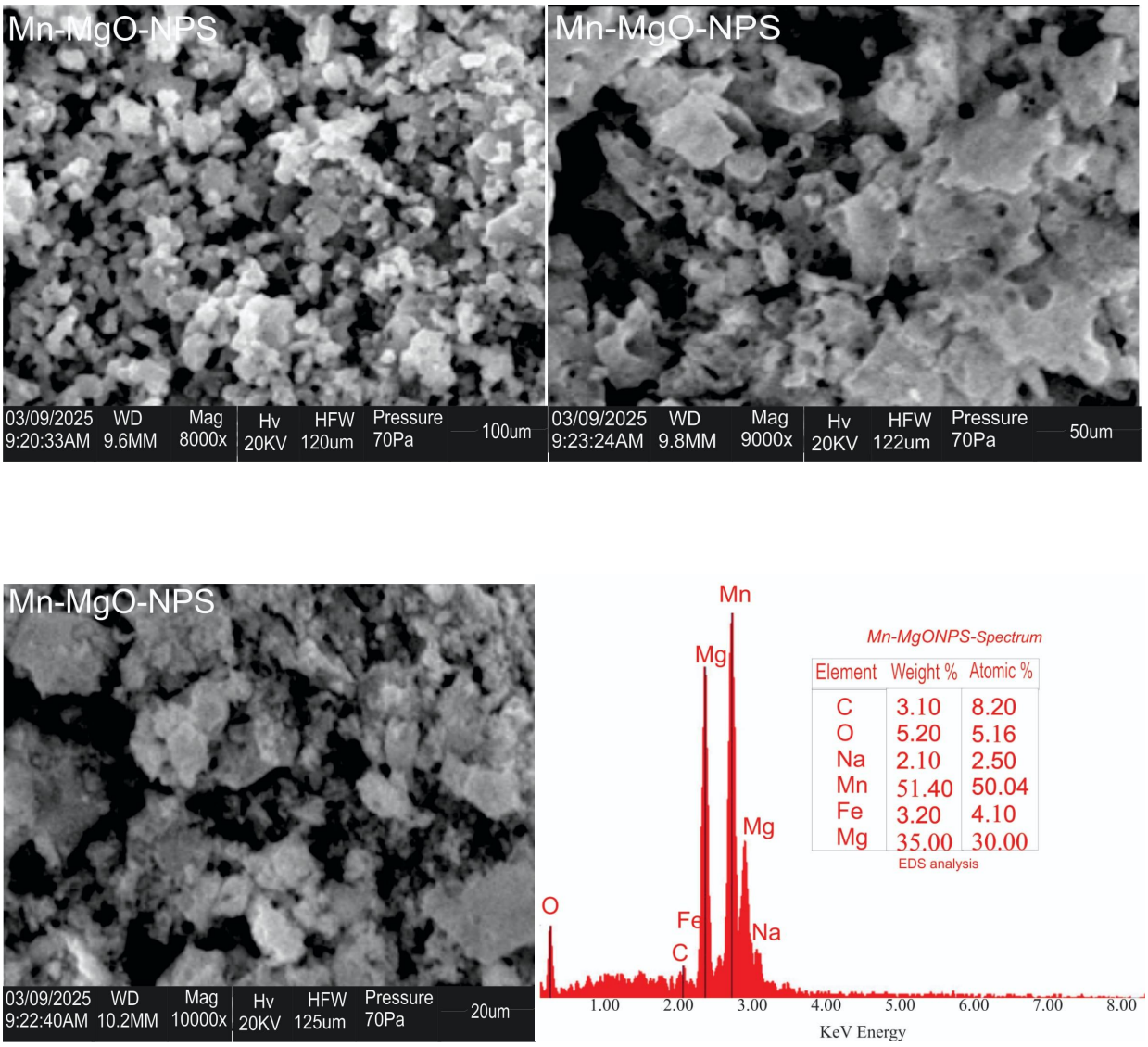

Fig 3.1 A: SEM micrograph at 100µm, B: SEM micrograph at 50µm, C: SEM micrograph at 20µm, D: EDS of Mn-MgO NPs.

3.3 X-RAY DIFFRACTION ANALYSIS

The phase, clarity, crystalline quality, and crystallographic structure of Mg-MnO NPs synthesized from aqueous *Ficus exasperata* extract were investigated using XRD. Figure 4 depicts three peaks with counts of 59, 104, and 91 for 2θ values of 29.4°, 42.9°, and 62.0°, respectively. Biosynthesized Mn-MgO NPs have a crystallographic structure, as indicated by peak positions at specified 2θ degrees. The existence of these strong and powerful peaks shows that plant-derived Mg-MnO NPs have a well-defined crystalline structure with specific

crystallographic orientation. The Debye-Scherrer equation was used to compute the crystalline size of NPs based on XRD results. The computation was based on the width of the largest peak (104) in XRD, situated at a 2θ value of 42.9°. The Scherrer equation is expressed as: D is the crystallite size, k is the form factor (often 1.5406Arm), is the X-ray wavelength, is the peak FWHM in radians, and is the Bragg angle measured in radians. The D value was calculated to be 18nm. Khan *et al*. (2021) obtained a comparable result from chemical synthesis via co-precipitation of Mn-Mg binary oxide nanoparticles, which had a crystallite size of 12.8nm.

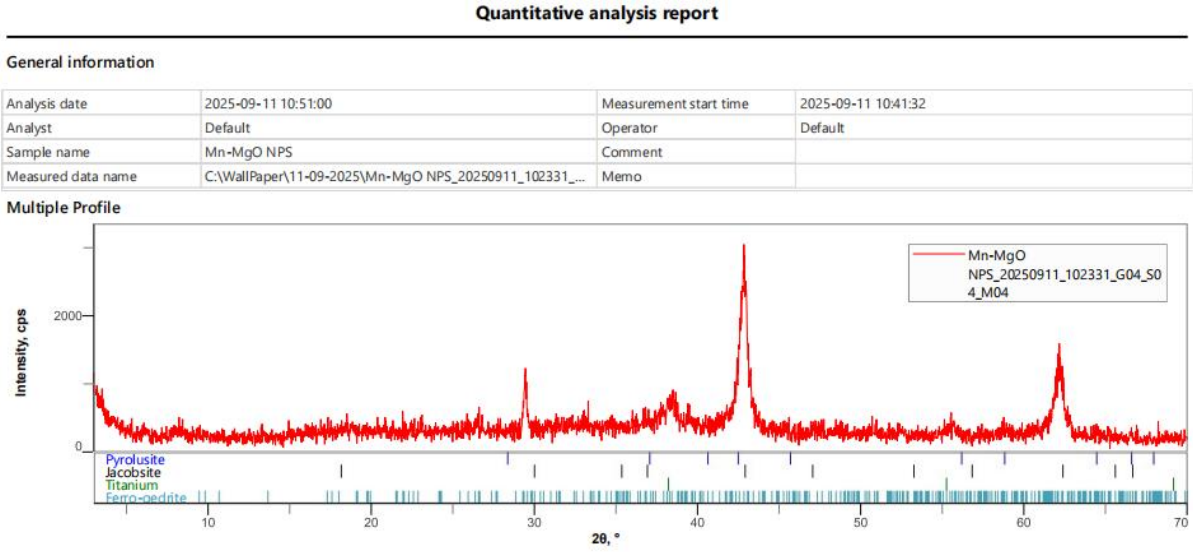

Fig 3.2 showing the X-RAY diffraction(XRD) analysis of Mn-MgO NPs

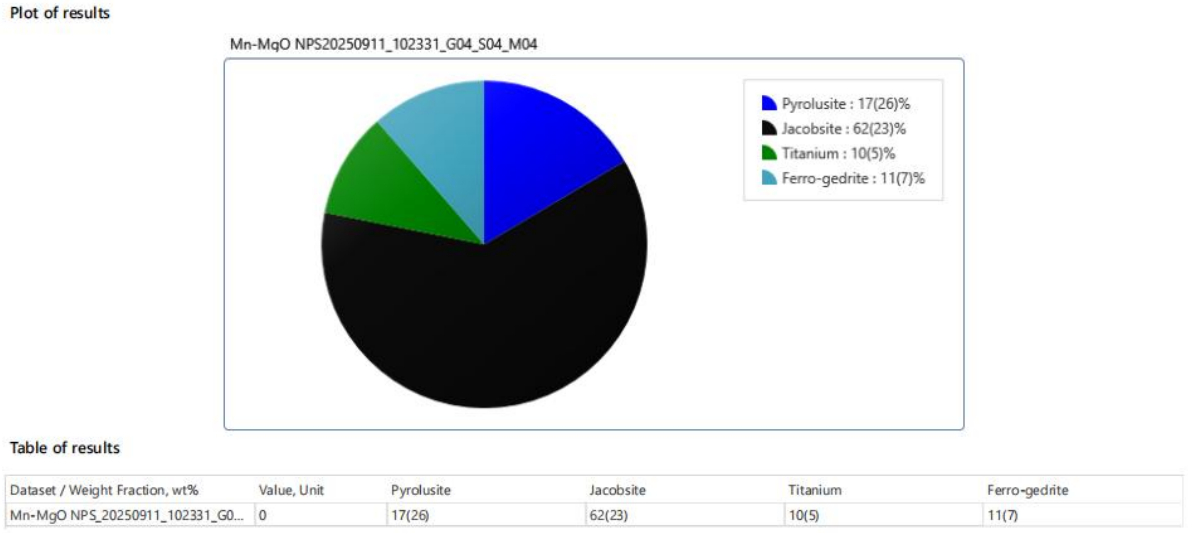

Fig 3.3:Pie Chart Showing Phase View Result of Different Fractions From XRD Analysis.

3.4 FT-IR (Fourier Transform Infrared Spectroscopy)

The FT-IR spectra of Mn-MgO nanoparticles produced with *Ficus exasperata* leaf extract displayed peaks at various wavenumbers. The produced nanoparticles' functional groups are identified using FT-IR spectroscopy, with spectra obtained in the 4000-650 cm^{-1} range. The first peak at 872.19 cm^{-1} corresponds to C-H out-of-plane bending vibrations present in organic molecules. The second peak at 928.11 cm^{-1} represents significant C=C stretching vibrations found in alkene groups. The band at 1017.5cm^{-1} corresponds to C-O stretching vibrations of esters, while the peak at 1408.93cm^{-1} corresponds to O-H bending, commonly associated with carboxylic acids, confirming the presence of organic residues from the *Ficus* extract. The absorption band at 1543.11 cm^{-1} could be attributed to aromatic C=C stretching or amide II vibrations, which includes N-H bending and C-N stretching. Furthermore, the absorption bands at 2344.49 cm^{-1} and 2374.31 cm^{-1} are attributed to O=C=O stretching, likely coming from the absorption of ambient CO_2 or CO_2 that is trapped or adsorbed on the surface of the nanoparticles. The broad band at 3339.69 cm^{-1} is related to O-H stretching vibrations, which may originate from alcoholic groups and hydrogen-bonded water molecules (Geentanjali *et al*., 2024). The FT-IR findings obtained here coincide with those reported for MgO nanoparticles generated using methanolic extracts of Sapindus mukorossi (reetha) by Geentanjali and colleagues (2024). It is worth noting that Mn-MgO nanoparticles were synthesized at low temperatures. Under these conditions, precursor molecules adsorbed on the nanoparticles' surfaces can have a considerable effect on the FT-IR spectra. As a result, the observed fluctuations in peak strength and small spectra shifts could be attributed to interactions between nanoparticles and their precursor molecules.

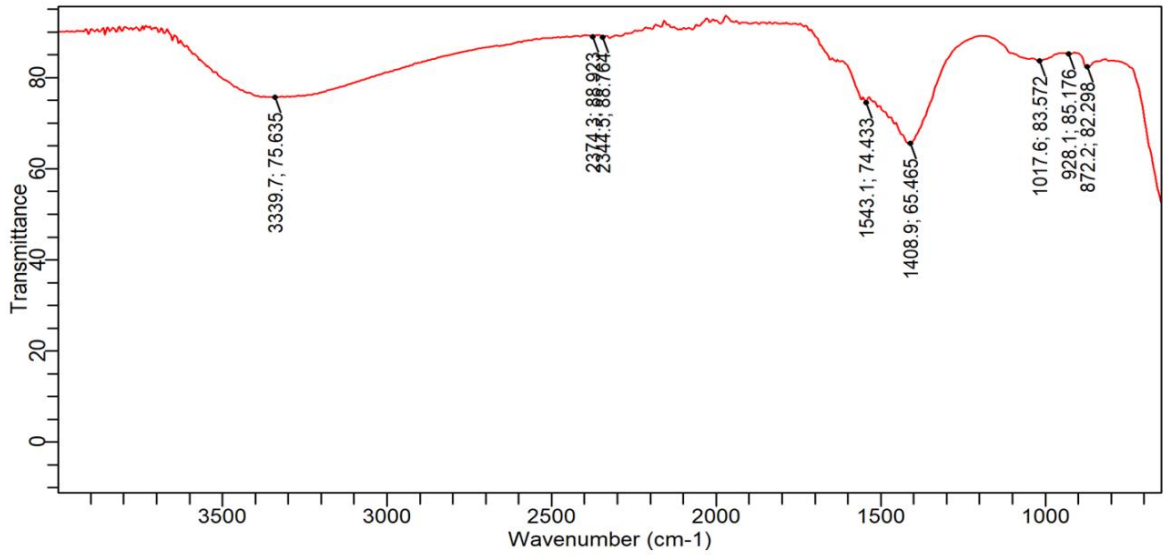

Figure 3.4 shows the FT-IR plot between wave number (cm^{-1}) and transmittance (%) of Mn-MgO using *Ficus exasperata* leaves extract.

Table 3.3: FTIR Peak Assignment for Mn-MgO binary oxide NPs formed.

Peak Number	Bands	Functional Group	Assignment
1	872.19705	C-H	Alkane group
2	928.10712	C=C	Alkene group
3	1017.56323	C-O	Esters
4	1408.93370	O-H	Alcohol
5	1543.11786	N-H	Secondary Amine
6	2344.49550	O=C=O	Carbon di oxide
7	2374.31420	O=C=O	Carbon di oxide
8	3339.69470	O-H	Alcoholic/Water molecule

3.5 **Brunauer-Emmett-Teller (BET)**

As seen in Fig. 1.5, nitrogen adsorption–desorption isotherms at 77 K were used to examine the surface characteristics of Mn–MgO nanoparticles. The BET evaluation revealed a comparatively high specific surface area of 212.13 m^2/g, indicating an abundance of active sites. The BJH approach estimated the overall pore volume to be approximately 0.106 cm^3/g, while the DFT and DR methods confirmed cumulative pore values of 0.0826 cm^3/g and 0.073 cm^3/g, respectively. A somewhat higher micropore volume of 0.186 cm^3/g was obtained using the DA approach, suggesting that the material has both micropores and mesopores. Nitrogen adsorption–desorption isotherms at 77 K were used to examine the surface characteristics of Mn–MgO nanoparticles. The analysis of the pore size distribution revealed that the Mn–MgO nanoparticles were primarily mesoporous, with average pore diameters of 2.11 nm (BJH method), 2.65 nm (DFT approach), and 3.04 nm (DA methodology). A slightly larger pore size of 5.67 nm was assessed through the DR method, which aligns with the existence of both micro- and mesoporous structures. Notably, a large micropore surface area of 205.6 m2/g was also found using the DR approach, indicating that microporous areas make up a sizable fraction of the total surface area. In conclusion, the nitrogen adsorption–desorption isotherm of Mn–MgO nanoparticles is categorized as a Type IV isotherm with an H3 hysteresis loop, which is typical of mesoporous materials with small apertures. These results demonstrated that the generated Mn–MgO nanoparticles have a large surface area, an appropriate pore volume, and a hybrid micro–mesoporous structure.

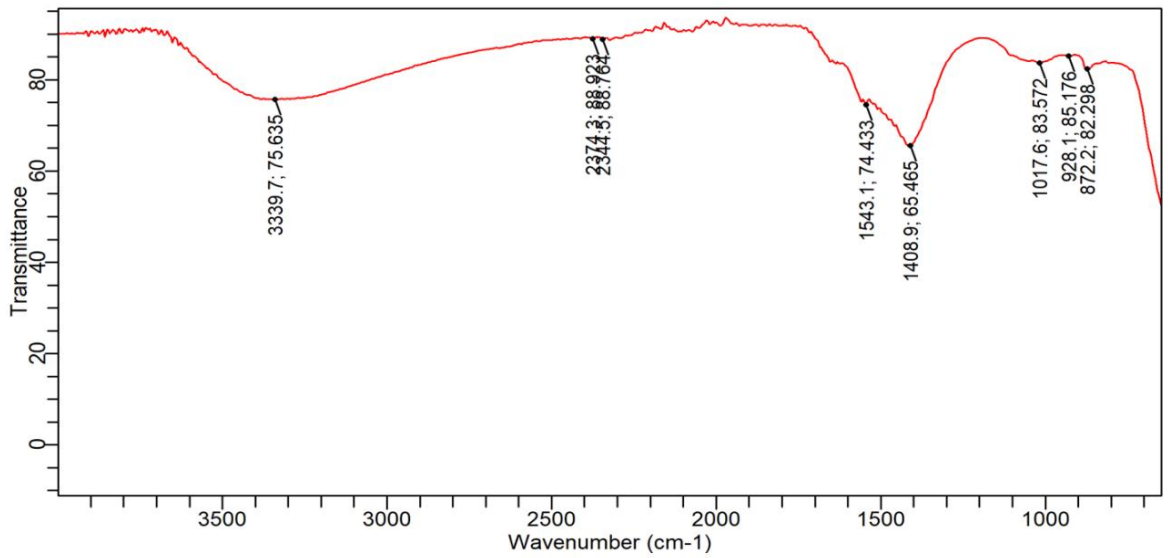

Fig. 3 .4 shows the **BET analysis plot** used to determine the **specific surface area** of Mn-MgO nanoparticles formed.

3.6 Antimicrobial Activity

Figure 3.5 depicts the antibacterial efficiency of green-synthesized Mn-MgO nanoparticles (NPs) against selected bacterial and fungal species such as *Bacillus subtilis, Staphylococcus aureus, Pseudomonas aeruginosa, Escherichia coli, Candida albicans, and Aspergillus niger*. The agar well diffusion technique was applied, with nanoparticle suspensions ranging in concentration from 62.5 to 7.813 mg/mL. After incubation for 24 hours at 37°C for bacteria and 48 hours for fungi, no obvious inhibitory zones were evident for any of the organisms tested at the quantities applied. As a result, the minimum inhibitory concentration (MIC) and minimum bactericidal/fungicidal concentration (MBC/MFC) were irrelevant because no inhibitory effects were detected. Under the experimental circumstances used in this study, Mn-MgO nanoparticles produced from *Ficus exasperata* leaf extract did not exhibit antibacterial efficacy against the pathogens tested. The unfavorable antimicrobial findings observed in this study contrast with various reports in existing literature where magnesium oxide (MgO) and manganese dioxide (MnO_2) nanoparticles synthesized separately have shown inhibitory effects on a broad range of microorganisms. For example, Raghupathi *et al*. (2011) noted that smaller ZnO and MgO nanoparticles (less than 50 nm) displayed considerable antibacterial activity through the production of reactive oxygen species (ROS) and the disruption of cell membranes. Likewise, Alavi *et al*. (2021) pointed out that MnO_2 nanostructures exhibited moderate antibacterial properties when suitably doped or modified on their surfaces. The lack of inhibition observed in this study may be due to several reasons:

Synergistic Effect of Binary Oxides: While binary oxides typically demonstrate improved properties, there are instances where the combination may diminish activity. Manganese oxides, in contrast to MgO, display variable antimicrobial effects, and their inclusion may have impacted the surface chemistry of the nanoparticles, leading to decreased reactivity.

Experimental and Environmental Factors: Factors such as the media's pH, the dispersion stability of nanoparticles, or inadequate interaction time with microbial cells might have restricted activity. Additionally, the concentrations studied (62.5–7.813 mg/mL), while relatively elevated, may not have been ideal for effective microbial inhibition.

Lack of Activation: Certain nanoparticles necessitate activation (for instance, under UV or visible light) to optimize ROS production and antimicrobial efficacy. Since the current research utilized dark incubation conditions, the inherent activity of Mn–MgO may not have been fully displayed. Even though antimicrobial activity was absent, this result remains important. It underscores the significance of synthesis conditions, the composition of plant extracts, and the physicochemical properties of nanoparticles in influencing biological functionality. Negative outcomes also add to the scientific knowledge surrounding nanomaterials by exposing limitations and highlighting the need for further optimization.

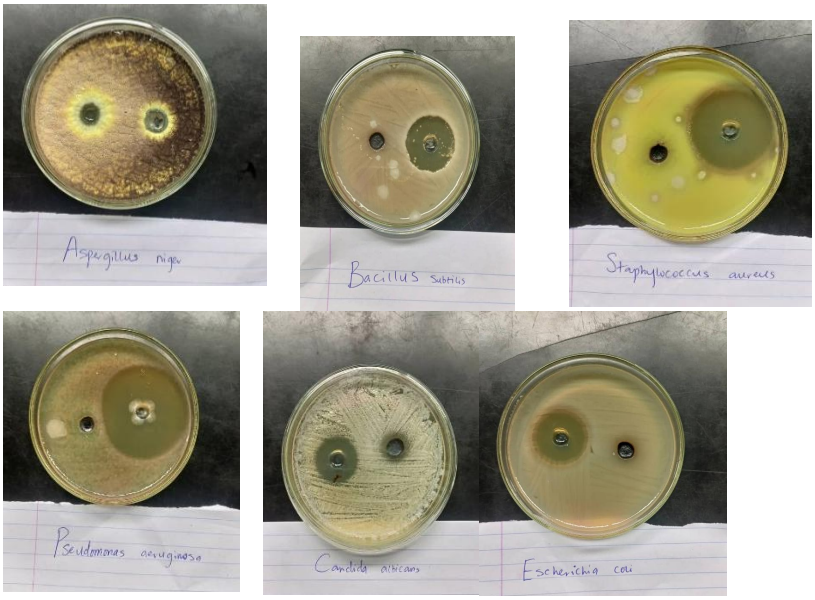

Plates 3.1 showing (a) Pseudomonas aeruginosa (b) Bacillus subtilis (c) Staphylococcus aureus (c) Aspergillus niger (d) Candida albicans (e) Escherichia coli bacterial culture of Mn-MgO NPs synthesized with *Ficus exasperata.*

CONCLUSION

This study successfully demonstrated the green synthesis of manganese–magnesium oxide nanoparticles (Mn–MgO NPs) using *Ficus exasperata* leaf extracts. The production of the nanoparticles was confirmed by characterization using SEM, EDS, XRD, and FTIR, which also demonstrated that phytochemicals functioned as stabilizing and reducing agents. However, antimicrobial evaluations against specific bacterial and fungal species, including *Aspergillus niger, Bacillus subtilis, Staphylococcus aureus, Pseudomonas aeruginosa, Escherichia coli, and Candida albicans*, showed no discernible inhibition under the investigated conditions. The absence of antibacterial efficacy emphasizes how important synthesis parameters, phytochemical composition, and nanoparticle physicochemical characteristics are in determining biological activity. Despite the disappointing results, they provide valuable scientific insights by identifying the limitations of using *Ficus exasperata* extracts for binary Mn–MgO synthesis.

REFERENCES

Ahmed, S., Ahmad, M., Swami, B. L., & Ikram, S. (2016). A review on plant extract-mediated synthesis of silver nanoparticles for antimicrobial applications: A green expertise. *Journal of Advanced Research, 7*(1), 17–28.

Alavi, M., Rai, M., & Martinez, F. (2021). Manganese oxide nanoparticles and their applications. *Applied Microbiology and Biotechnology, 105*(2), 473–486.

Hamza, A., Mohamed, R. M., & Abdullah, A. M. (2021). Binary metal oxide nanomaterials for environmental and biomedical applications. *Journal of Materials Science, 56*(12), 7502–7518.

Ikhuoria, E. U., Aigbodion, S. J., & Okoye, C. O. (2021). Antimicrobial potentials of biogenic nanoparticles. *Journal of Applied Sciences and Environmental Management, 25*(5), 793–802.

Jobby, R., Jha, P., Yadav, A. K., & Desai, N. (2018). Biosynthesis of nanoparticles using eco-friendly factories and their role in plant–pathogen interaction. *Biotechnology Reports, 19*, e00268.

Kobelnik, M., de Oliveira, A. C., & Júnior, P. I. (2021). Phytochemical-assisted synthesis of nanoparticles: Mechanisms and applications. *Environmental Nanotechnology, Monitoring & Management, 16*, 100576.

Krishnamoorthy, K., Manivannan, G., Kim, S. J., Jeyasubramanian, K., & Premanathan, M. (2012). Antibacterial activity of MgO nanoparticles based on lipid peroxidation by oxygen vacancy. *Journal of Nanoparticle Research, 14*(9), 1063.

Kumar, R., Umar, A., Kumar, G., & Nalwa, H. S. (2020). Antimicrobial properties of metal oxides and their applications in biomedical, food, and environmental sectors. *Chemical Reviews, 120*(19), 887–950.

Mittal, A. K., Chisti, Y., & Banerjee, U. C. (2013). Synthesis of metallic nanoparticles using plant extracts. *Biotechnology Advances, 31*(2), 346–356.

Okoye, T. C., Akah, P. A., Ezike, A. C., Onyeto, C. A., & Nworu, C. S. (2014). Ficus exasperata Vahl (Moraceae): A review of its pharmacological and phytochemical properties. *International Journal of Phytomedicine, 6*(2), 324–331.

Rafique, M., Sadaf, I., Rafique, M. S., & Tahir, M. B. (2022). Role of morphology and size of nanoparticles in antimicrobial activity. *Materials Science and Engineering: C, 127*, 112199.

Raghupathi, K. R., Koodali, R. T., & Manna, A. C. (2011). Size-dependent bacterial growth inhibition and mechanism of antibacterial activity of zinc oxide nanoparticles. *Langmuir, 27*(7), 4020–4028.

Salata, O. (2004). Applications of nanoparticles in biology and medicine. *Journal of Nanobiotechnology, 2*, 3.

Salem, S. S., Fouda, A., & Fouda, H. M. (2019). Green synthesis of magnesium oxide nanoparticles: Applications in antimicrobial activity. *Journal of Cluster Science, 30*(6), 1425–1434.

Selim, Y. A., Azb, M. A., Ragab, I., & Abd El-Azim, M. H. (2021). Green synthesis and characterization of silver nanoparticles using aqueous extract of *Ricinus communis* seeds. *Journal of Nanostructure Chemistry, 11*(1), 111–121.

Song, P., Zhang, Y., & Ding, Y. (2018). Antibiotic resistance in pathogens and its mechanisms. *Journal of Global Antimicrobial Resistance, 13*, 47–54.

Ebiaguanye, I. T., & Emeribe, F. O. (2024). Biosynthesis of Magnesium Oxide Nanoparticles using Pennisetum Purpureum and Application in Removal of Cadmium Contaminant from Water.*Dutse Journal of Pure and Applied Sciences*,*10*(1c), 21-33.

WHO (2020). Antimicrobial resistance. *World Health Organization*. Retrieved from https://www.who.int/news-room/fact-sheets/detail/antimicrobial-resistance

APPENDIX

APPENDIX I

Quantachrome NovaWin - Data Acquisition and Reduction
for NOVA instruments
©1994-2013, Quantachrome Instruments
version 11.03

Analysis			Report			
Operator:	**Abdulrahman Abdulkareem**	**Date: 2025/09/04**	**Operator: Abdulrahman Abdulkareem**		**Date: 2025/09/04**	
Sample ID:	Mn-MgO NPs	**Filename:**	Mn-MgO NPs.qps			
Sample Desc:		**Comment:**				
Sample weight:	0.3 g	**Sample Volume:**	1 cc			
Outgas Time:	3.0 hrs	**OutgasTemp:**	250.0 C			
Analysis gas:	Nitrogen	**Bath Temp:**	273.0 K			
Press. Tolerance:	0.100/0.100 (ads/des)	**Equil time:**	60/60 sec (ads/des)	**Equil timeout:**	240/240 sec (ads/des)	
Analysis Time:	114.0 min	**End of run:**	**2025/08/26 15:03:35**	**Instrument:**	Nova Station B	
Cell ID:	2					

DA Plot

Data Reduction Parameters

DA Method	**Incr. E:**	500.000	**Incr. n:**	0.100	**Interact. Const. (K):**	2.960nm³ x kJ / mol
Adsorbate	**Nitrogen**		**Temperature**	77.350K		
	Molec. Wt.:	28.013	**Cross Section:**	16.200 Å²	**Liquid Density:**	0.808 g/cc

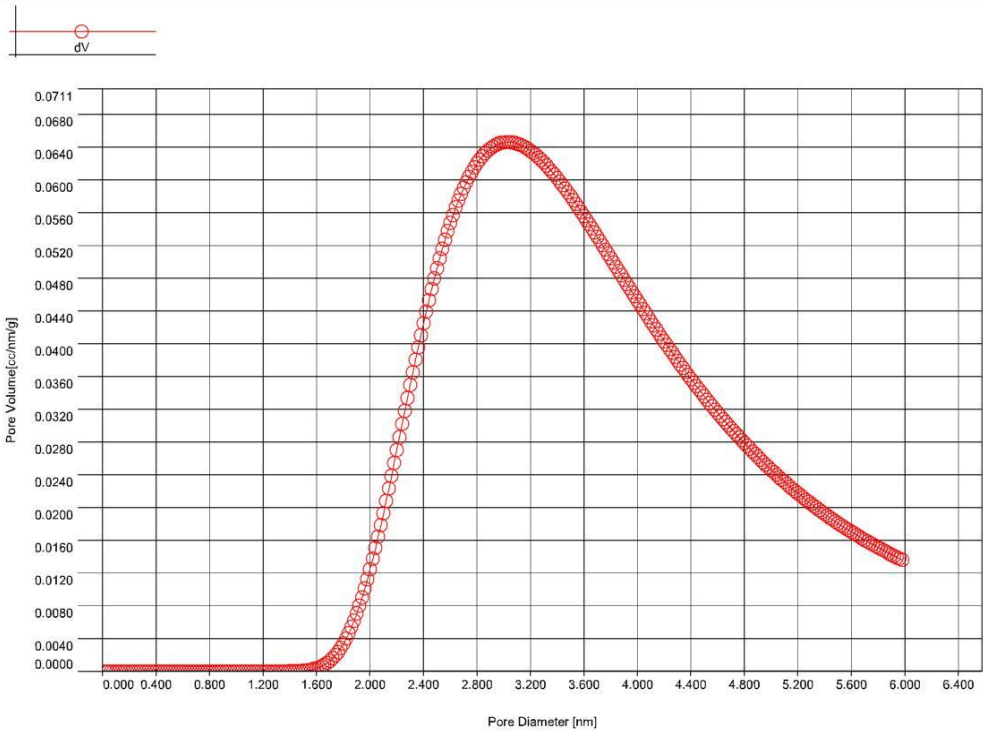

DA method summary

Best E =	0.638 kJ/mol
Best n =	1.000
DA Micropore Volume =	0.186 cc/g
Pore Diameter (mode)=	3.040e+00 nm

APPENDIX II

Quantachrome NovaWin - Data Acquisition and Reduction
for NOVA instruments
©1994-2013, Quantachrome Instruments
version 11.03

Analysis			Report			
Operator:	**Abdulrahman Abdulkareem**	**Date: 2025/09/04**	**Operator: Abdulrahman Abdulkareem**		**Date: 2025/09/04**	
Sample ID:	Mn-MgO NPs	**Filename:**	Mn-MgO NPs.qps			
Sample Desc:		**Comment:**				
Sample weight:	0.3 g	**Sample Volume:**	1 cc			
Outgas Time:	3.0 hrs	**OutgasTemp:**	250.0 C			
Analysis gas:	Nitrogen	**Bath Temp:**	273.0 K			
Press. Tolerance:	0.100/0.100 (ads/des)	**Equil time:**	60/60 sec (ads/des)	**Equil timeout:**	240/240 sec (ads/des)	
Analysis Time:	114.0 min	**End of run:**	**2025/08/26 15:03:35**	**Instrument:**	Nova Station B	
Cell ID:	2					

BJH method Adsorption dV(d)

Data Reduction Parameters

t-Method	**Calc. method:** de Boer						
BJH/DH method	**Moving pt. avg.:** off						
Adsorbate	**Nitrogen**		**Temperature**	77.350K			
	Molec. Wt.: 28.013		**Cross Section:**	16.200 A²	**Liquid Density:**	0.808 g/cc	

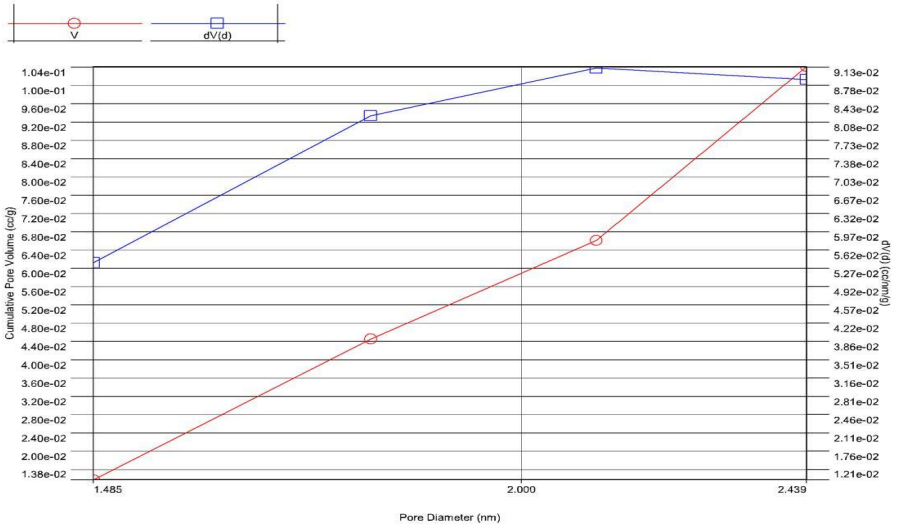

BJH adsorption summary

Surface Area =	208.782 m²/g
Pore Volume =	0.104 cc/g
Pore Diameter Dv(d) =	2.107 nm

APPENDIX III

Table 3.1: Results Obtained Using Scherrer Equation For All Peaks Using K= 0.9 and = 1.5406Å

Peaks	2θ	FWHM (°)	D (nm)
1	9.23	2.70	2.98
2	29.42	0.20	39.77
3	38.22	0.65	12.35
4	42.85	0.50	17.12
5	55.53	0.66	12.04
6	62.02	0.62	13.00

Table 3.2: RESULTS OBTAINED FROM XRD ANALYSIS

PEAK	2θ	FWHM (°)	D (nm)
1	9.23	2.70	3.10
2	29.42	0.20	43.50
3	38.22	0.65	13.60
4	42.85	0.50	18.00
5	55.53	0.66	14.20
6	62.02	0.62	15.50